

Original Article

LUNG CANCER-ASSOCIATED MESENCHYMAL STEM CELLS MEDIATE CHEMORESISTANCE AND MALIGNANT PROGRESSION OF LUNG CANCER THROUGH ACTIVATING HIF-1 α

L.B. Pang^{1,2}, J. Li¹, Z.W. Zhang^{3,*} and C.Q. Zhang^{2,4,*}¹Department of Pulmonary and Critical Care Medicine, Jinan Central Hospital, 250013 Jinan, Shandong, China²Cheeloo College of Medicine, Shandong University, 250013 Jinan, Shandong, China³Department of Radiology, Shandong Provincial Hospital Affiliated to Shandong First Medical University, 250021 Jinan, Shandong, China⁴Department of Pulmonary and Critical Care Medicine, Shandong Provincial ENT Hospital, 250000 Jinan, Shandong, China

Abstract

Background: The high mortality of lung cancer is mainly attributed to not only late detection and diagnosis but also strong invasion and the potential development of chemoresistance. This study investigated the effect and underlying mechanisms of mesenchymal stem cells (MSCs) isolated from lung cancer tissues (LC-MSCs) on lung cancer progression and chemoresistance. **Methods:** LC-MSCs were isolated using tissue culture method. They were characterized and verified through microscopic observation via flow cytometry (for determining MSC expression markers) and testing their ability of differentiation into adipose cells, osteocytes, or chondrocytes. Then, lung cancer A549 and H1299 cell lines cultured alone or co-cultured with LC-MSCs were used for exploring how LC-MSCs affect the progression of lung cancer cells. Temozolomide (TMZ) was administrated on differently cultured cells to determine how LC-MSCs affect the chemoresistance of lung cancer cells. Cell proliferation was evaluated by cell counting kit-8 assay, and cell cycle distribution was assessed by flow cytometry. Cell invasion, migration, and apoptosis were determined by Transwell assay, wound healing assay, and flow cytometry, respectively. Reverse transcription quantitative polymerase chain reaction, Western blot, and immunofluorescence were used to verify the upregulation of hypoxia-inducible factor-1 α (HIF-1 α) by LC-MSCs, and HIF-1 α expression was mediated by transfection to investigate the effect of HIF-1 α on lung cancer cell progression and chemoresistance. The effects of LC-MSCs and HIF-1 α on autophagy-related LC3-II/I ratio, Beclin-1, p62, and epithelial-mesenchymal transition (EMT)-related N-cadherin and E-cadherin were measured. Nude BALB/c mice were subcutaneously injected with lung cancer cells or LC-MSCs co-cultured with lung cancer cells. They were also administrated with or without TMZ. The tumor volume, tumor weight, and levels of HIF-1 α , LC3-II/I ratio, Beclin-1, p62, E-cadherin and N-cadherin, proliferation (Ki-67 immunohistochemistry), and apoptosis (terminal deoxynucleotidyl transferase-mediated dUTP nick end labeling (TUNEL) assay) of the formed lung cancer tumor tissues were measured. **Results:** Under or under no TMZ administration, LC-MSCs promoted cell proliferation, migration, and invasion and inhibited cell apoptosis ($p < 0.01$). When co-cultured with LC-MSCs, HIF-1 α was more expressed in cells ($p < 0.01$). Under or under no TMZ administration, HIF-1 α increased proliferation, migration, invasion, autophagy, and EMT and decreased the apoptosis of cells co-cultured with LC-MSCs ($p < 0.01$). In mice treated with TMZ, LC-MSCs and HIF-1 α promoted tumor growth in terms of volume and weight, proliferation, autophagy, and EMT in tumor cells and inhibited cell apoptosis ($p < 0.01$). **Conclusions:** LC-MSCs promote the malignant progression of lung cancer and enhance cancer cell resistance to chemotherapy through upregulating HIF-1 α expression, thus providing new targets of LC-MSCs and HIF-1 α for lung cancer treatment.

Keywords: Mesenchymal stem cells, lung cancer, HIF-1 α , chemoresistance, temozolomide.

***Address for correspondence:** C.Q. Zhang, Cheeloo College of Medicine, Shandong University, 250013 Jinan, Shandong, China; Department of Pulmonary and Critical Care Medicine, Shandong Provincial ENT Hospital, 250000 Jinan, Shandong, China. Email: freezcq66@163.com; Z.W. Zhang, Department of Radiology, Shandong Provincial Hospital Affiliated to Shandong First Medical University, 250021 Jinan, Shandong, China. Email: sduzzw@163.com.

Copyright policy: © 2025 The Author(s). Published by Forum Multimedia Publishing, LLC. This article is distributed in accordance with Creative Commons Attribution Licence (<http://creativecommons.org/licenses/by/4.0/>).

Introduction

Lung cancer has become not only the most frequent cancer but also the leading cause of cancer-related mortality in North America and other countries as well as in men and women combined [1–3]. The late detection of lung cancer is the number one main cause of high mortality and poor overall survival rates [4,5]. Another main cause inducing poor overall survival is the disease's malignant progression [6]. Lung cancer has caused many deaths due to its strong invasion and the potential to develop drug resistance [7]. The responses of patients with lung cancer to chemotherapy are often not long-lasting, and chemotherapy resistance could be easily developed, resulting in disease exaggeration and recurrence [8,9]. Therefore, exploring the progression and chemoresistance mechanisms of lung cancer and identifying therapeutic targets are crucial.

Mesenchymal stem cells (MSCs) were first uncovered in 1976 [10]. Various cell lineages, including adipocytes, chondrocytes, and osteocytes, can be differentiated from this type of widely distributed and multipotent cells [11,12]. MSCs can be isolated from various tissues, and they possess the expression markers CD90, CD73, CD105, and CD166 [13,14]. A notable detail is that MSCs could strongly modulate immune response and affect the development of numerous types of diseases, including cancers [15–17]. MSCs may emit either suppressive or promotive effect on cancer progression [18]. However, studies investigating lung cancer-associated mesenchymal stem cells (LC-MSCs) and their effect on human lung cancer are few [19]. In spite of a previous study claiming that the porcine lung MSCs possessed properties of immunoregulation [20] and LC-MSCs promoted tumorigenesis and tumor metastasis of lung cancer [19], the role of LC-MSCs in lung cancer progression and the underlying mechanisms should be explored and verified further.

Hence, in this study, the effect of LC-MSCs on the malignant progression and chemoresistance development of human lung cancer was investigated, and the underlying signaling pathway was explored. The findings may help evaluate MSC-based anti-lung cancer therapies for clinical application and improving the life quality of patients with lung cancer.

Materials and Methods

LC-MSC Preparation

LC-MSCs were isolated from primary lung cancer tissues, which were obtained from five patients with lung cancer and by surgical section in Jinan Central Hospital. They were immediately immersed in phosphate-buffered saline (PBS; 10010002, Gibco, Grand Island, NY, USA) containing 1 % penicillin/streptomycin (15140148, Gibco, Grand Island, NY, USA) at 4 °C. MSCs were isolated within 4 h after the tissues were obtained. When performing isolation, the remaining blood was removed by rins-

ing tissues with ice-cold PBS, and the tissues were cut into 8 mm³ blocks, with vessels in tissues being completely removed. These blocks were plated on culture flasks, which was pre-moistened with Dulbecco's modified Eagle medium/Nutrient Mixture F-12 (DMEM/F-12; 11039021, Gibco, Grand Island, NY, USA) containing 2 mmol/L L-glutamine (21051024, Gibco, Grand Island, NY, USA) and 10 % fetal bovine serum (FBS; 16140071, Gibco, Grand Island, NY, USA). The flasks were placed upside down in humidified atmosphere containing 5 % CO₂, and the blocks were incubated overnight at 37 °C. Then, 1 mL of medium was added into the flasks in the morning of the second, third, and fourth days, and 3 mL of medium was added into the flasks in the morning of the fifth day. For every 3 days, half of the medium was changed. After 2 weeks, the isolated MSCs were passaged (at 65 %–70 % confluence) by being trypsinized using 0.25 % trypsin and 1 mM ethylenediaminetetraacetic acid (AM9260G, Invitrogen, Carlsbad, CA, USA) at room temperature, and the floating cells were collected. The MSCs were cultured at a density of 4 × 10³ cells/cm² and used for subsequent experiments at 4–6 passages. The LC-MSCs were mycoplasma-free, and short tandem repeat (STR) analysis revealed that they were derived from parental cells.

LC-MSC Characterization and Identification

The morphological characterization and phenotype of isolated LC-MSCs were observed under a microscope (CKX53, Olympus, Tokyo, Japan) and identified using flow cytometry to detect surface markers, respectively. In brief, cells in 70 % confluence were trypsinized, rinsed with PBS, and suspended (10⁷/mL). At room temperature, the cells were stained with antibodies of CD73 (ab288154), CD90 (ab288825), CD105 (ab221675), CD29 (ab193591), CD14 (ab182032), CD34 (ab8536), CD45 (ab218503), and HLA-DR (ab136320) separately. All these antibodies were purchased from Abcam (Cambridge, MA, USA) and used with a 1:500 dilution. The cells were incubated on ice for 30 min, washed with PBS, centrifugated for 5 min at 1800 rpm, suspended with PBS (500 μL), and then tested by flow cytometry (FACS Aria III, BD Bioscience, San Jose, CA, USA).

LC-MSC Multi-Differentiation

For adipogenic differentiation, LC-MSCs at 70 %–80 % confluence were cultured in DMEM/F-12 containing 10 % FBS, 1 % penicillin/streptomycin, 0.2 mM indomethacin, 1 μM dexamethasone, and 10 μg/mL insulin for 21 days, with medium being refreshed every 3 days. The LC-MSCs were stained with Oil Red O (C1957S, Beyotime, Shanghai, China), and adipogenesis was observed by microscope (CKX53, Olympus, Tokyo, Japan). For osteogenic differentiation, the LC-MSCs were cultured in DMEM/F-12 containing 10 % FBS, 1 % penicillin/streptomycin, 0.05 mM L-ascorbic acid-2-phosphate, 100 nM dexamethasone, and 10 mM β-glycerophosphate

for 21 days, with medium being refreshed every 3 days. All these medium contents were provided in the CellsStem-Pro osteogenesis differentiation kit (A1007201, Gibco, Grand Island, NY, USA). The LC-MSCs were stained with Alizarin Red S (C0148S, Beyotime, Shanghai, China), and osteogenesis was observed under the microscope. For adipogenic differentiation, the StemPro Lipogenesis differentiation kit (A1007001, Gibco, Grand Island, NY, USA) was used for culture, and Oil Red O (G1262, Solarbio, Beijing, China) was used for staining. For chondrogenic differentiation, the LC-MSCs were cultured in DMEM/F-12 containing 10 % FBS, 1 % penicillin/streptomycin, insulin, transferrin, selenium, 10 mM β -glycerophosphate, 10 nM dexamethasone, 0.05 mM L-ascorbic acid-2-phosphate, and 10 ng/mL transforming growth factor (TGF)- β 3 for 21 days, with medium being refreshed every 3 days. All these medium contents were provided in the chondrogenic differentiation kit (A1007101, Gibco, Grand Island, NY, USA). The LC-MSCs were stained with Alcian Blue (C0153S, Beyotime, Shanghai, China), and osteogenesis was observed under the microscope.

Cell Culture

The human lung cancer cell lines of A549 (iCell-h011) and H1299 (iCell-h153) were purchased from iCell Bioscience Inc. (Shanghai, China) and cultured in DMEM (iCell-0001, iCell Bioscience Inc.) containing 1 % penicillin/streptomycin and 10 % FBS. The cells were incubated at 37 °C under 5 % CO₂ and humidity. For co-culturing, the lung cancer cells were co-cultured with LC-MSCs (10:1) in Thermo Scientific Nunc plates (141006, Thermo Scientific, Shanghai, China), in which the LC-MSCs were seeded on the bottom layer of each well, and the lung cancer cells were maintained in the upper layer of the plate. Then, the cells were administrated with temozolomide (TMZ; HY-17364, MedChemExpress, Monmouth Junction, NJ, USA) for 24 h at a certain concentration. The lung cancer cells cultured alone were termed as mo.A549 and mo.H1299, and the lung cancer cells cultured with LC-MSCs were termed as co.A549 and co.H1299. The cells were tested without contamination with mycoplasma. The A549 and H1299 cells were mycoplasma-free, and STR analysis revealed that they were derived from parental cells.

Cell Transfection

For regulation of stable expression, lentivirus encoding short hairpin (sh)RNA of hypoxia-inducible factor-1 α (HIF-1 α) (sh-HIF-1 α ; 5'-CCATCCAGAGTCACTGGAAC-3'), noncoding shRNA (shNC), overexpression HIF-1 α (OE-HIF-1 α), or OE-NC were constructed by GeneChem (Shanghai, China) and transduced into A549 or H1299 cells following the manufacturer's instruction. At 48 h after transfection, the successful infection was selected by puromycin (2 μ g/mL), and the transfection efficiency was verified by

real-time reverse transcription quantitative polymerase chain reaction (RT-qPCR) and Western blot.

Cell Viability Assay

Cells were seeded onto 96-well plates (1 \times 10⁴ cells/well) with different treatments as designed and cultured for 48 h. Then, the lung cancer cells cultured alone or with LC-MSCs were collected, added with cell counting kit (CKK)-8 solution (10 μ L) (C0038, Beyotime, Shanghai, China), and subsequently incubated for 2 h. The absorbance at 450 nm was determined using a microplate reader (Multiskan SkyHigh, Thermo Fisher Scientific, Shanghai, China).

Flow Cytometry Analysis for Cell Apoptosis and Cell Cycle

Cell apoptosis was carried out using the Annexin V-FITC apoptosis detection kit (C1062M, Beyotime, Shanghai, China). Lung cancer cells were collected, digested, centrifugated, washed, rinsed, and resuspended with Annexin V-FITC and propidium (PI) provided by the apoptosis assay kit (C1062M, Beyotime, Shanghai, China). After 20 min in the dark, cell apoptosis was analyzed by flow cytometry (FACS Aria III, BD Bioscience, San Jose, CA, USA).

Cells were collected, washed with PBS, and fixed in 70 % cold ethanol overnight. At least 5 \times 10⁴ cells were stained by PI, and cell cycle was analyzed by fluorescence-activated cell sorting flow cytometry (FACS Aria III, BD Bioscience, San Jose, CA, USA).

Wound Healing Assay

Cells were seeded onto six-well plates as designed with different treatments and at the density of 5 \times 10⁵ cells/well. When the cells formed a single layer through adhesion, a scratch on the plate was made using a pipetting tip. The wound area was photographed under the microscope (CKX53, Olympus, Tokyo, Japan) at 0 and 24 h after scratching and analyzed by ImageJ software (version 1.35, NIH, Bethesda, MD, USA).

$$R_m = \frac{W_i - W_f}{W_f} \quad (1)$$

R_m : rate of cell migration; W_i : initial wound area; W_f : final wound area.

Transwell Assay

Cells were cultured in FBS-free DMEM (100 μ L) and added in the top chamber of 24-well plates (5 \times 10⁴ cells/well) containing 8 μ m-pore polycarbonate filter membrane. The bottom chamber was supplemented with 20 % FBS as a chemoattractant. The upper compartment was pre-coated with or with no Matrigel (0.2 %; 356234, BD Bioscience, San Jose, CA, USA) for invasion or migration assay, respectively. After 24 h of incubation, the

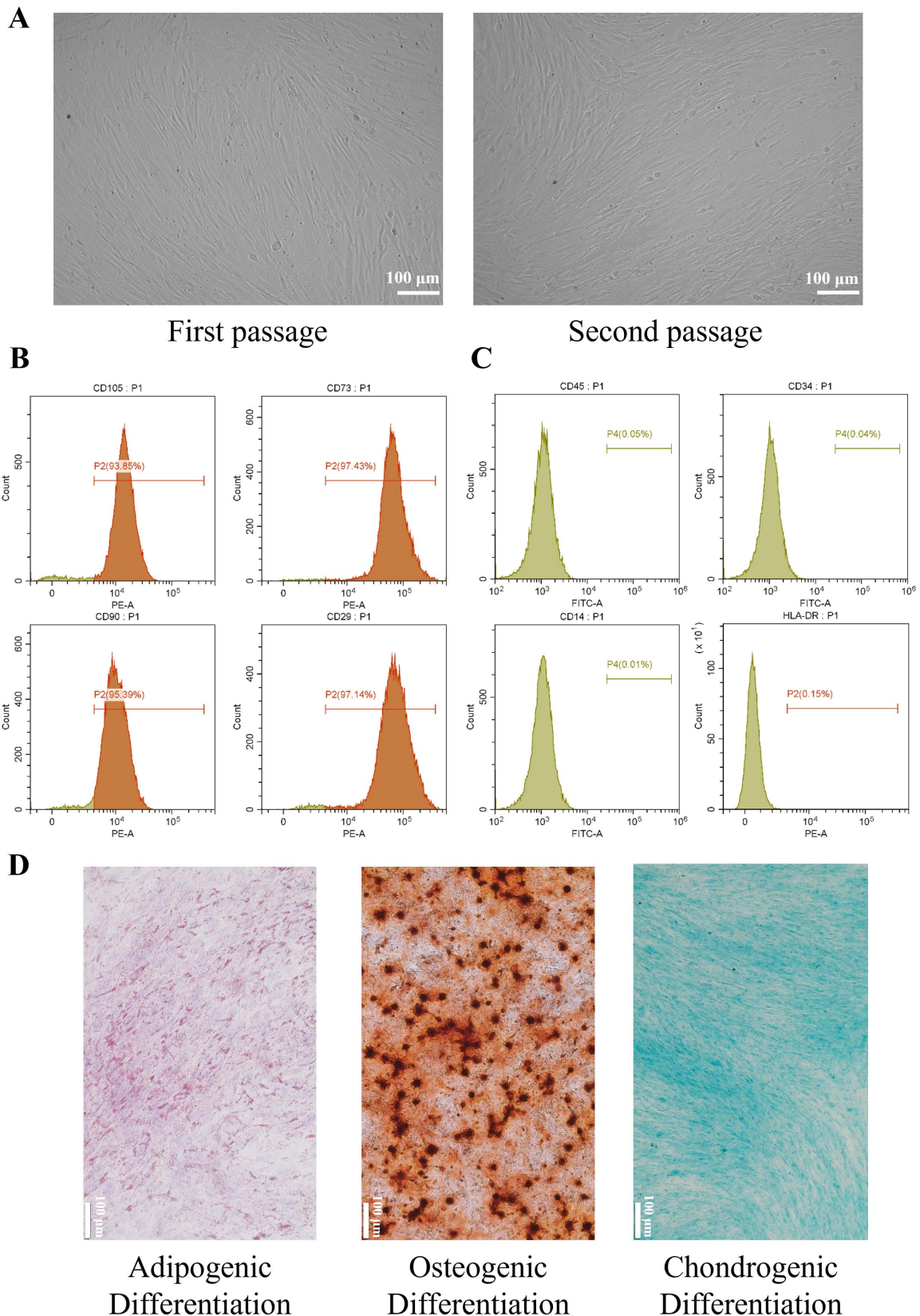


Fig. 1. Verification of isolated lung cancer-associated mesenchymal stem cells (LC-MSCs). (A) Morphology of LC-MSCs at first passage (left) and second passage (right). Scale bar: 100 μm . Expression levels of (B) MSC surface markers and (C) hematopoietic markers in LC-MSCs as tested by flow cytometry. (D) Adipogenic, osteogenic, and chondrogenic differentiations of LC-MSCs induced *in vitro*. Scale bar: 100 μm . MSCs, mesenchymal stem cells.

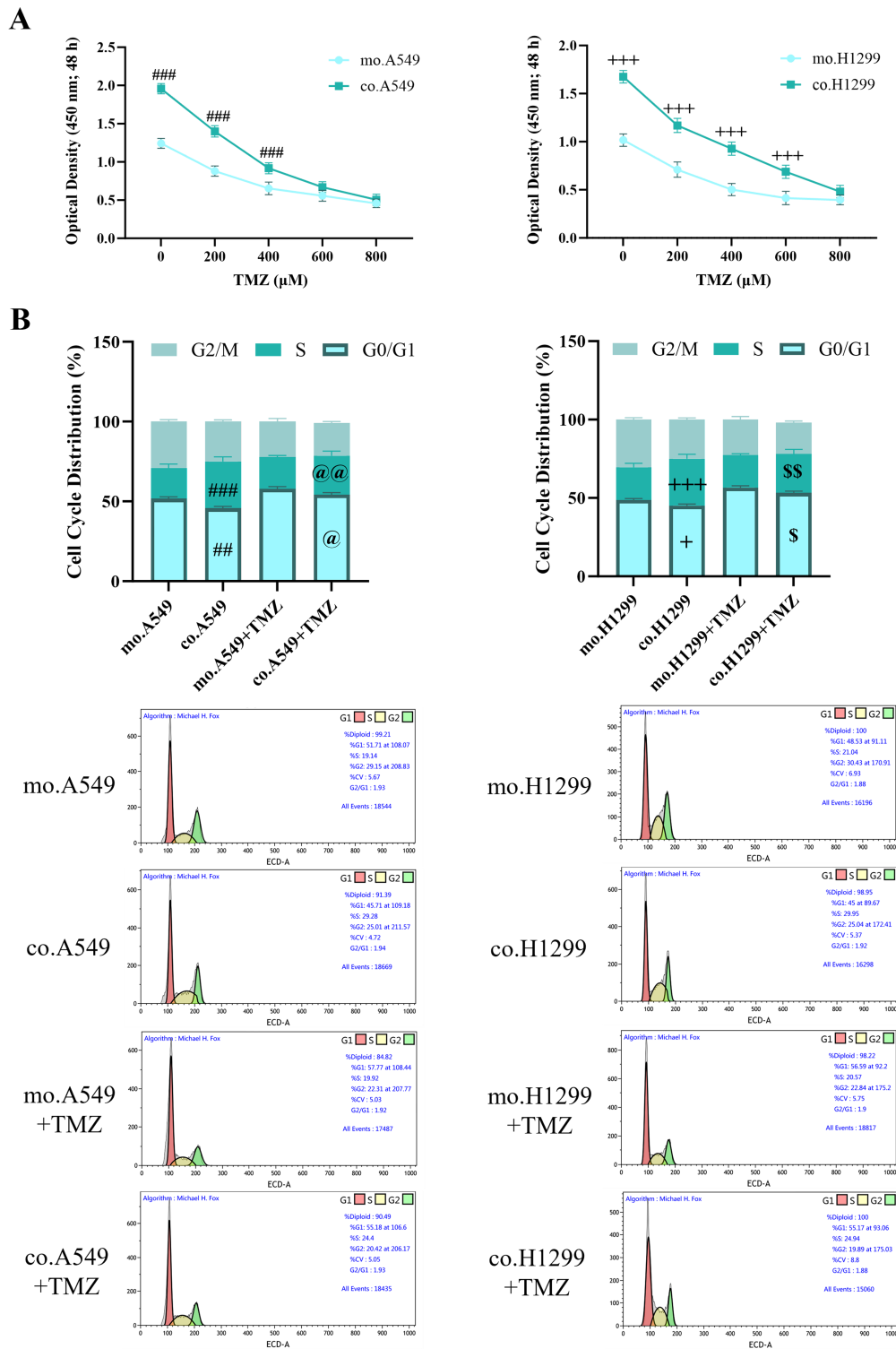


Fig. 2. Increase in the progression and chemoresistance of lung cancer cells by LC-MSCs. (A) Cell viability ($n = 5$). **(B)** Distribution of cell cycle ($n = 5$). mo.A549: A549 cells cultured alone; co.A549: A549 cells co-cultured with LC-MSCs; mo.A549 + TMZ: A549 cells cultured alone treated with $200 \mu\text{M}$ TMZ; co.A549 + TMZ: A549 cells co-cultured with LC-MSCs treated with $200 \mu\text{M}$ TMZ; mo.H1299: H1299 cells cultured alone; co.H1299: H1299 cells co-cultured with LC-MSCs; mo.H1299 + TMZ: H1299 cells cultured alone treated with $200 \mu\text{M}$ TMZ; and co.H1299+ TMZ: H1299 cells co-cultured with LC-MSCs treated with $200 \mu\text{M}$ TMZ. $\#\#p < 0.01$, $\#\#\#p < 0.001$ versus mo.A549; $@p < 0.05$, $@@p < 0.01$ versus mo.A549 + TMZ; $+p < 0.05$, $+++p < 0.001$ versus mo.H1299; $sp < 0.05$, $$$p < 0.01$ versus mo.H1299 + TMZ. TMZ, temozolomide.

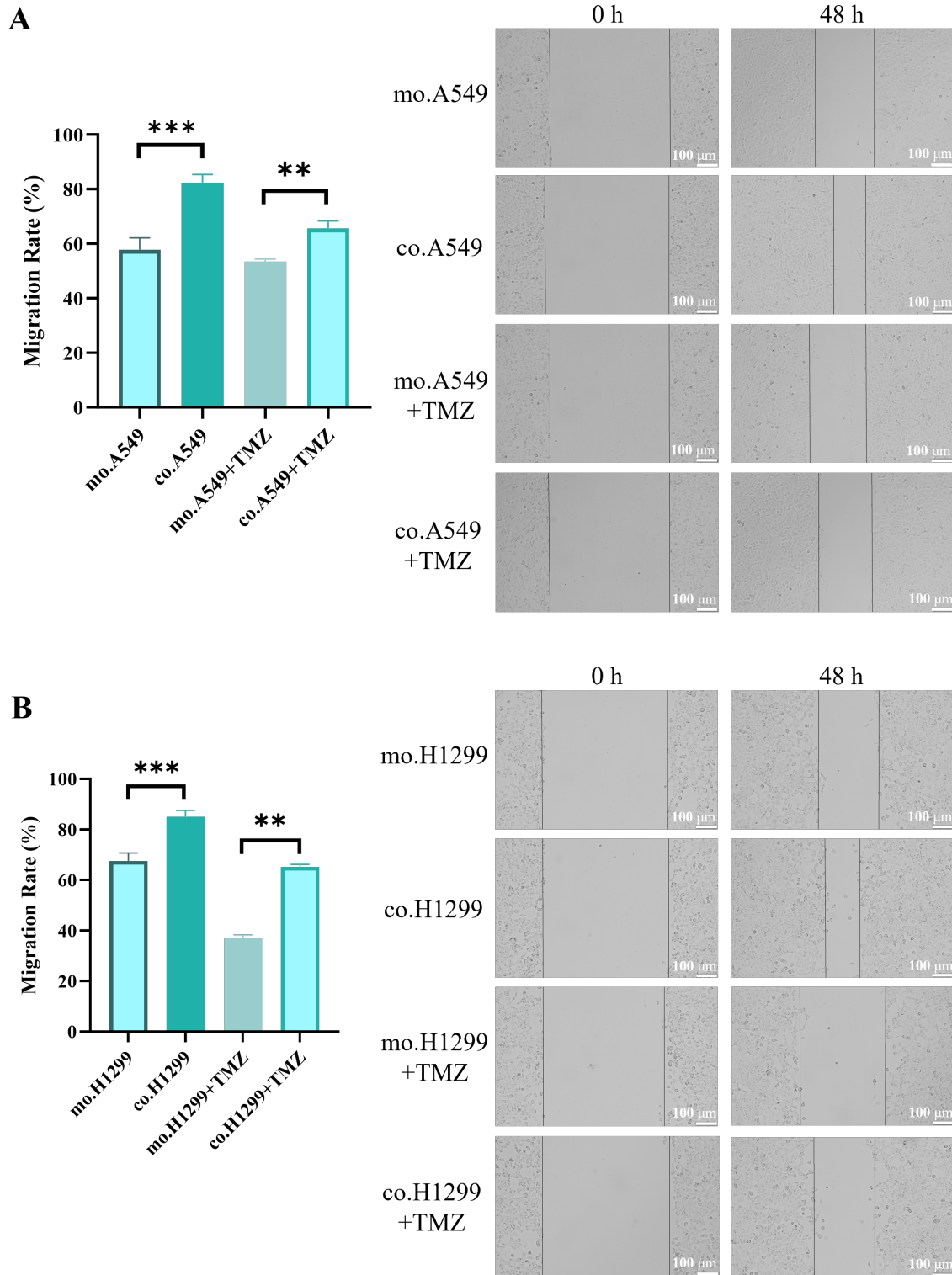


Fig. 3. Increase in the progression and chemoresistance of lung cancer cells by LC-MSCs. (A) Results of wound healing assay of A549 cells. (B) Results of wound healing assay of A1299 cells. (n = 5). Scale bar: 100 μm . mo.A549: A549 cells cultured alone; co.A549: A549 cells co-cultured with LC-MSCs; mo.A549 + TMZ: A549 cells cultured alone treated with 200 μM TMZ; co.A549 + TMZ: A549 cells co-cultured with LC-MSCs treated with 200 μM TMZ; mo.H1299: H1299 cells cultured alone; co.H1299: H1299 cells co-cultured with LC-MSCs; mo.H1299 + TMZ: H1299 cells cultured alone treated with 200 μM TMZ; and co.H1299+ TMZ: H1299 cells co-cultured with LC-MSCs treated with 200 μM TMZ. ** $p < 0.01$, *** $p < 0.001$.

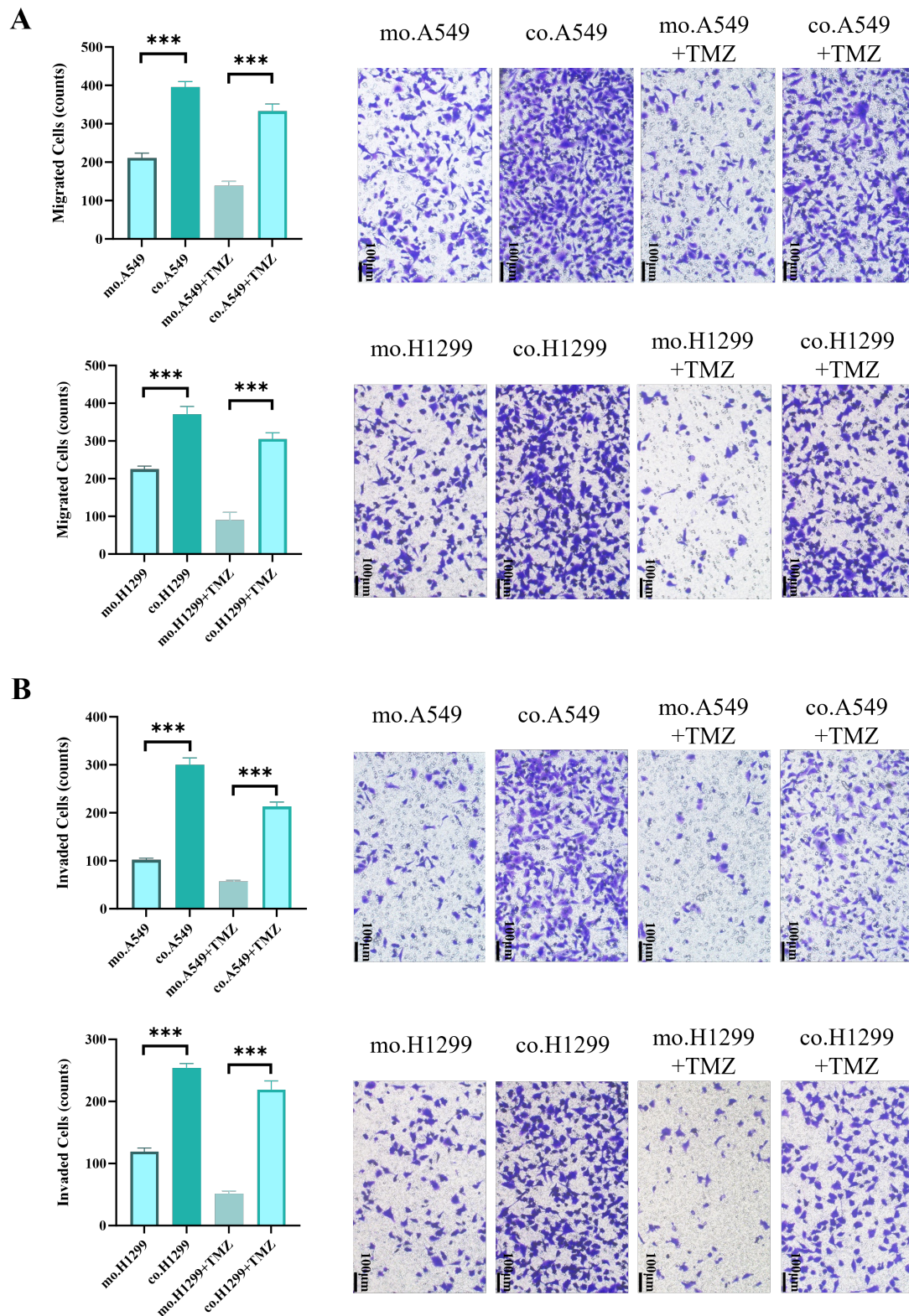


Fig. 4. Increase in the progression and chemoresistance of lung cancer cells by LC-MSCs. Results of Transwell assays for (A) migration and (B) invasion ($n = 5$). Scale bar: $100 \mu\text{m}$. mo.A549: A549 cells cultured alone; co.A549: A549 cells co-cultured with LC-MSCs; mo.A549 + TMZ: A549 cells cultured alone treated with $200 \mu\text{M}$ TMZ; co.A549 + TMZ: A549 cells co-cultured with LC-MSCs treated with $200 \mu\text{M}$ TMZ; mo.H1299: H1299 cells cultured alone; co.H1299: H1299 cells co-cultured with LC-MSCs; mo.H1299 + TMZ: H1299 cells cultured alone treated with $200 \mu\text{M}$ TMZ; and co.H1299 + TMZ: H1299 cells co-cultured with LC-MSCs treated with $200 \mu\text{M}$ TMZ. *** $p < 0.001$.

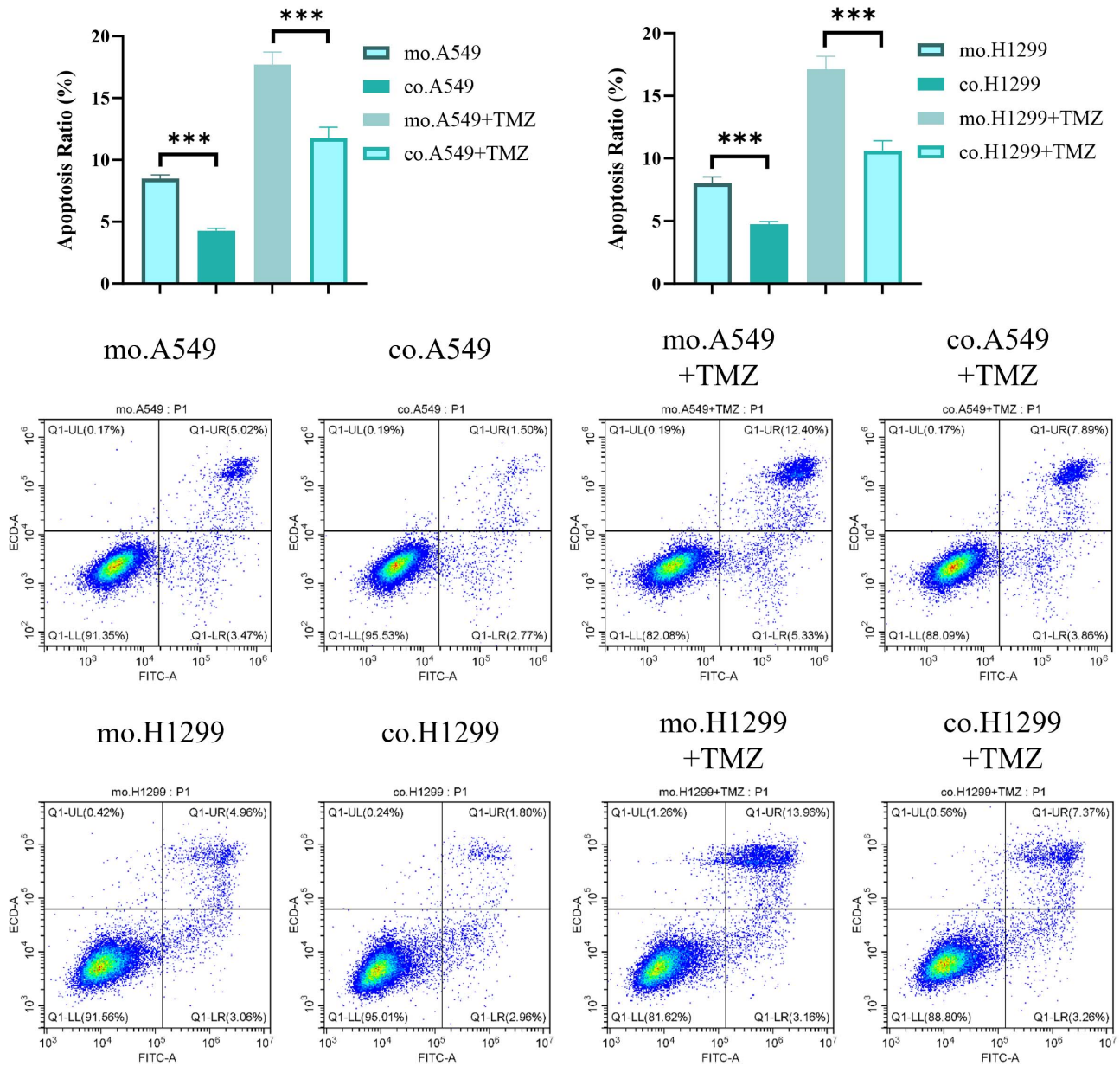


Fig. 5. Increase in the progression and chemoresistance of lung cancer cells by LC-MSCs. Results of apoptosis obtained by flow cytometry (n = 5). mo.A549: A549 cells cultured alone; co.A549: A549 cells co-cultured with LC-MSCs; mo.A549 + TMZ: A549 cells cultured alone treated with 200 μ M TMZ; co.A549 + TMZ: A549 cells co-cultured with LC-MSCs treated with 200 μ M TMZ; mo.H1299: H1299 cells cultured alone; co.H1299: H1299 cells co-cultured with LC-MSCs; mo.H1299 + TMZ: H1299 cells cultured alone treated with 200 μ M TMZ; and co.H1299 + TMZ: H1299 cells co-cultured with LC-MSCs treated with 200 μ M TMZ. ****p* < 0.001.

cells on the lower surface of the filter were fixed with 4 % paraformaldehyde (P0099, Beyotime, Shanghai, China), stained with crystal violet (C0121, Beyotime, Shanghai, China), and calculated under the microscope (CKX53, Olympus, Tokyo, Japan).

Immunofluorescence

Cells with different treatments were collected and seeded on a dish. Then, they were treated with

paraformaldehyde (0.4 %; C0121, Beyotime, Shanghai, China) and Triton X-100 (0.3 %; P0096, Beyotime, Shanghai, China). Next, the cells were incubated with the primary antibody for HIF-1 α (1:200 dilution, ab1, Abcam, Cambridge, MA, USA) overnight and the allogeneic secondary antibody (1:500 dilution, ab96879, Abcam, Cambridge, MA, USA) in the dark for 1 h. The nuclei were stained with 2-(4-amidinophenyl)-6-indolecarbamide dihydrochloride (DAPI; C1002, Beyotime, Shanghai, China). Afterwards,

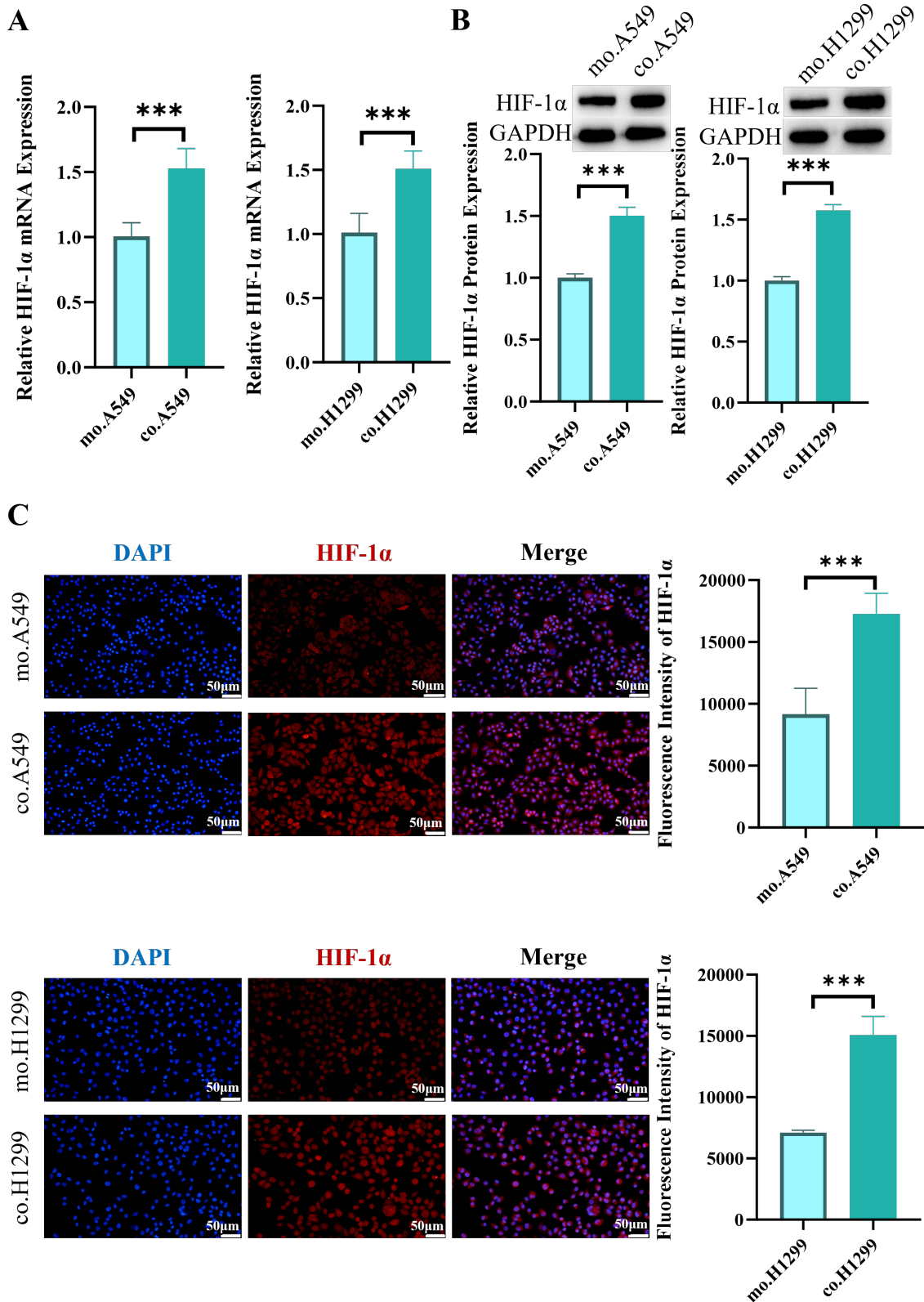


Fig. 6. Upregulation of HIF-1 α expression by LC-MSCs. (A) HIF-1 α mRNA expression and (B) HIF-1 α protein expression (n = 5). (C) Immunofluorescence analysis of HIF-1 α expression (n = 5). Scale bars: 50 μ m. mo.A549: A549 cells cultured alone; co.A549: A549 cells co-cultured with LC-MSCs; mo.H1299: H1299 cells cultured alone; and co.H1299: H1299 cells co-cultured with LC-MSCs. *** p < 0.001. HIF-1 α , hypoxia-inducible factor-1 α ; GAPDH, glyceraldehyde-3-phosphate dehydrogenase; DAPI, 2-(4-amidinophenyl)-6-indolecarbamide dihydrochloride.

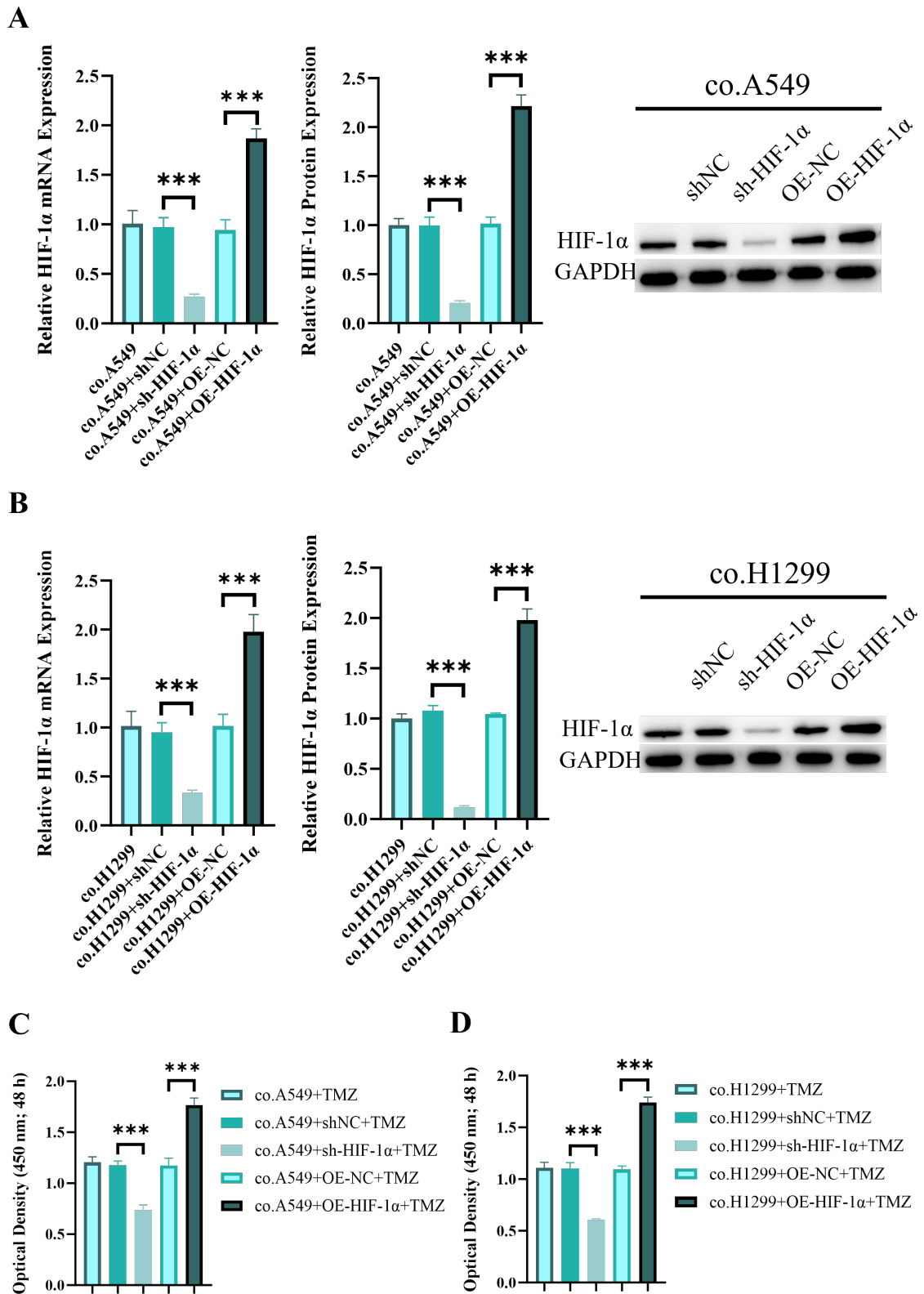


Fig. 7. LC-MSC enhancement of chemoresistance in lung cancer cells through upregulating HIF-1 α . mRNA expression of HIF-1 α obtained by RT-qPCR (n = 5) and protein expression obtained by Western blot (n = 5) in (A) transfected A549 cells and (B) transfected H1299 cells. Results of CCK-8 assays (n = 5) for (C) transfected A549 cells and (D) transfected H1299 cells co-cultured with LC-MSCs and treated with TMZ. *** $p < 0.001$. RT-qPCR, reverse transcription quantitative polymerase chain reaction; CCK, cell counting kit; sh, short hairpin; shNC, noncoding shRNA; OE, overexpression.

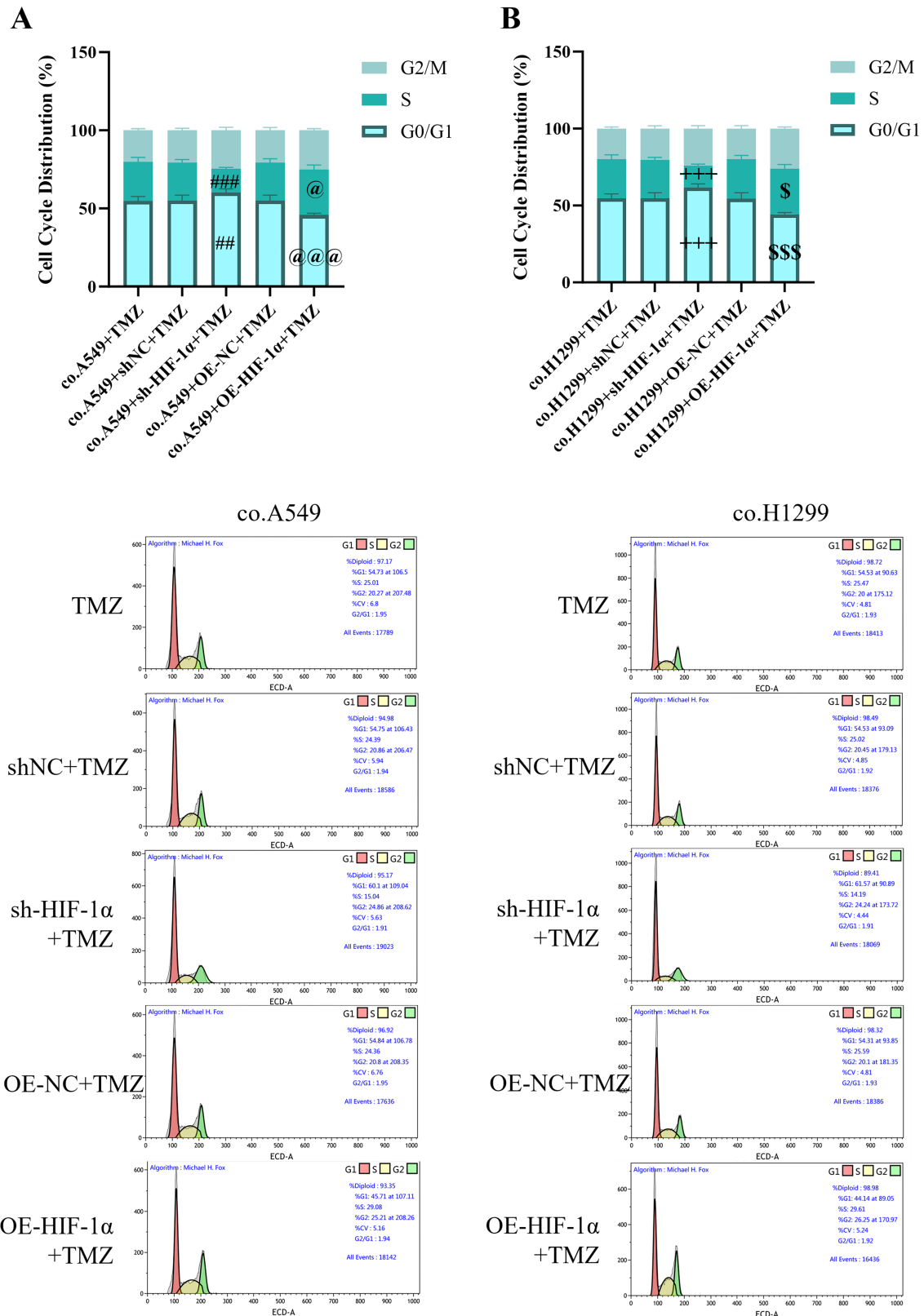


Fig. 8. LC-MSC enhancement of chemoresistance in lung cancer cells through upregulating HIF-1 α . Cell cycle distribution obtained by flow cytometry (n = 5) in (A) transfected A549 cells and (B) transfected H1299 cells co-cultured with LC-MSCs and treated with TMZ. ## $p < 0.01$, ### $p < 0.001$ versus co.A549 + shNC + TMZ. @ $p < 0.05$, @@@ $p < 0.001$ versus co.A549 + OE-NC + TMZ. +++ $p < 0.001$ versus co.H1299 + shNC + TMZ. \$ $p < 0.05$, \$\$\$ $p < 0.001$ versus co.H1299 + OE-NC + TMZ.

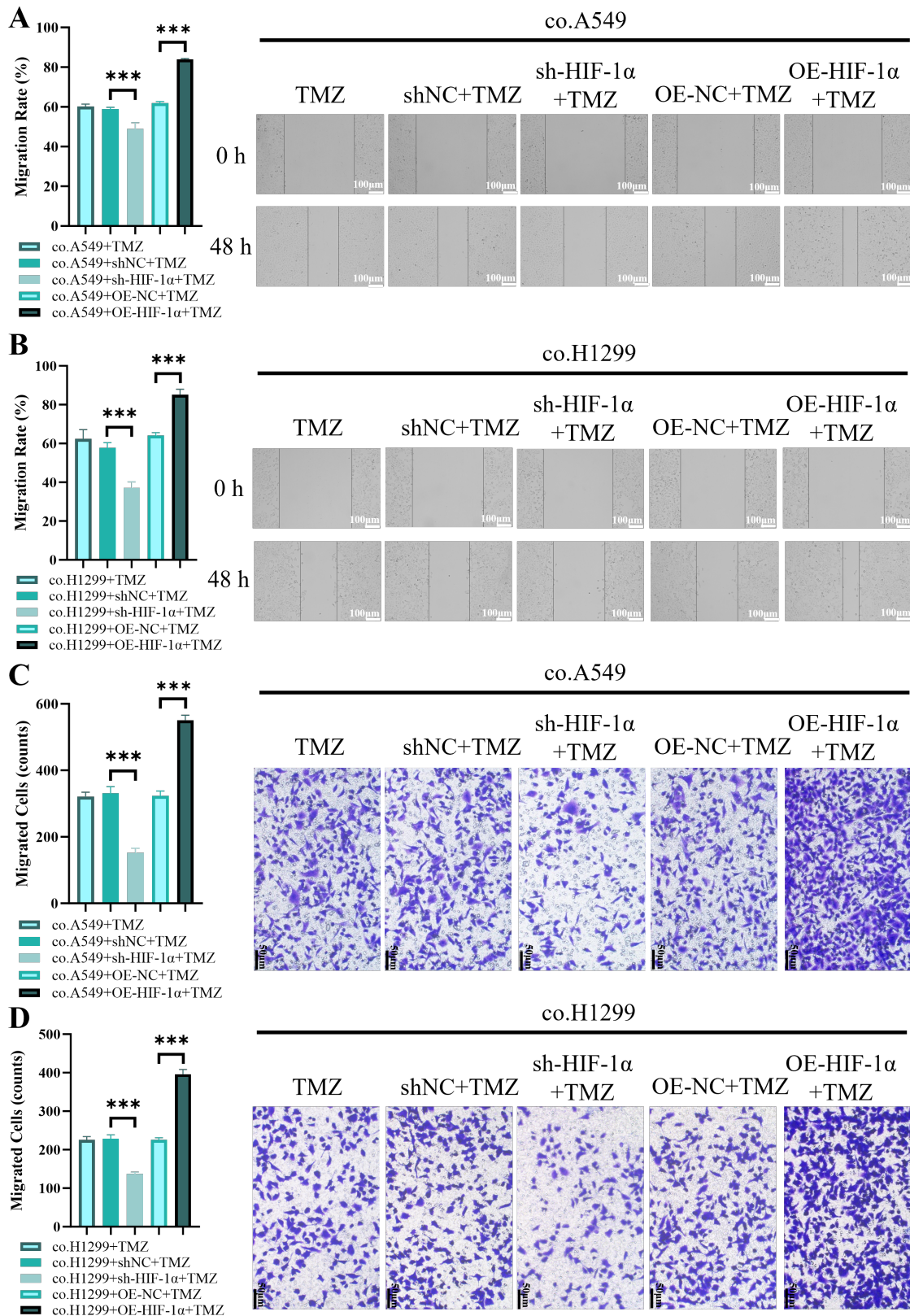


Fig. 9. LC-MSC enhancement of chemoresistance in lung cancer cells through upregulating HIF-1 α . Wound healing assays ($n = 5$; scale bar: 100 μm) for (A) transfected A549 cells and (B) transfected H1299 cells co-cultured with LC-MSCs and treated with TMZ. Transwell migration assays ($n = 5$; scale bar: 50 μm) for (C) transfected A549 cells and (D) transfected H1299 cells co-cultured with LC-MSCs and treated with TMZ. *** $p < 0.001$.

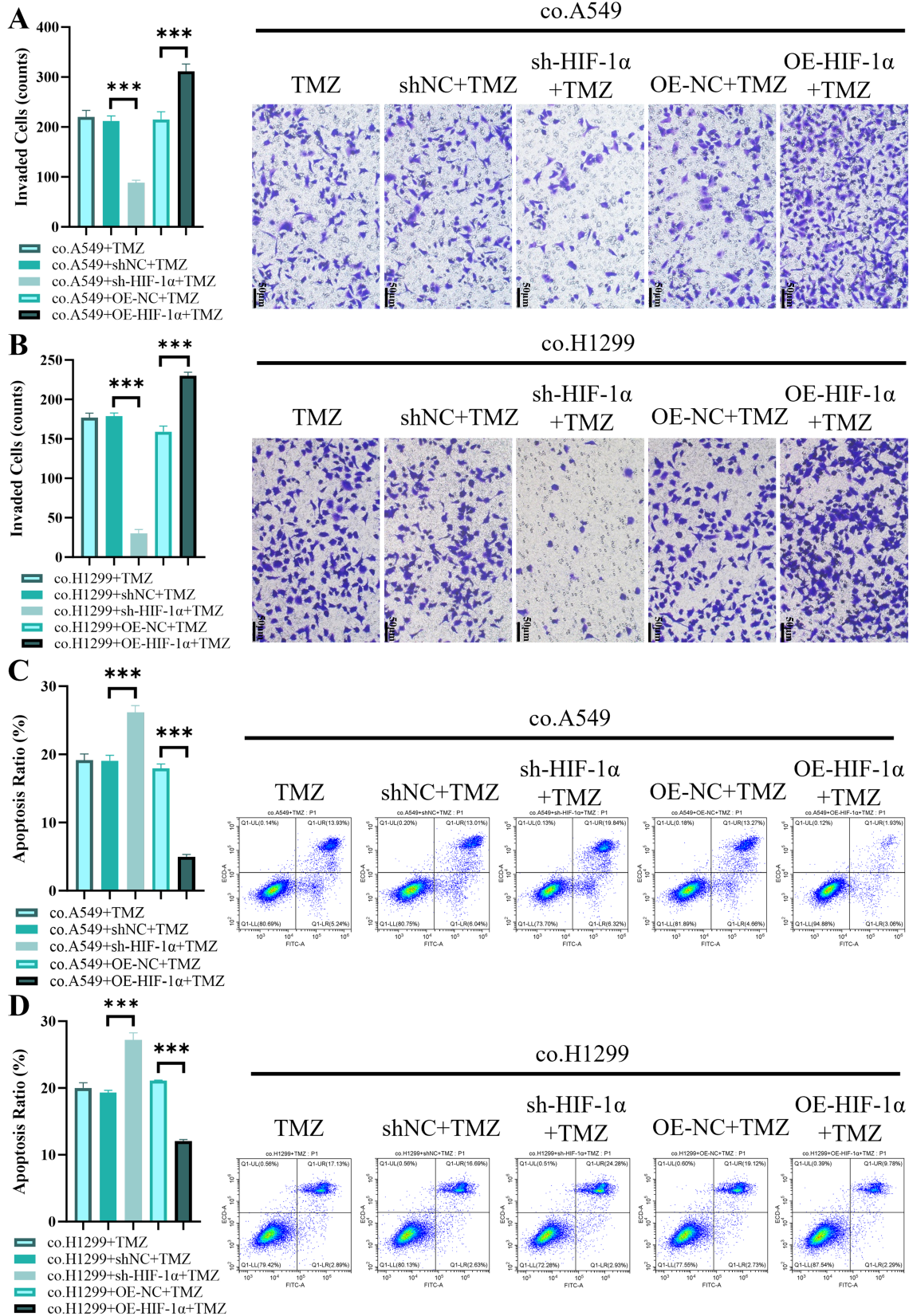


Fig. 10. LC-MSC enhancement of chemoresistance in lung cancer cells through upregulating HIF-1 α . Transwell invasion assays ($n = 5$; scale bar: 50 μm .) for (A) transfected A549 cells and (B) transfected H1299 cells co-cultured with LC-MSCs and treated with TMZ. Apoptosis examined via flow cytometry ($n = 5$) of (C) transfected A549 cells and (D) transfected H1299 cells co-cultured with LC-MSCs and treated with TMZ. $***p < 0.001$.

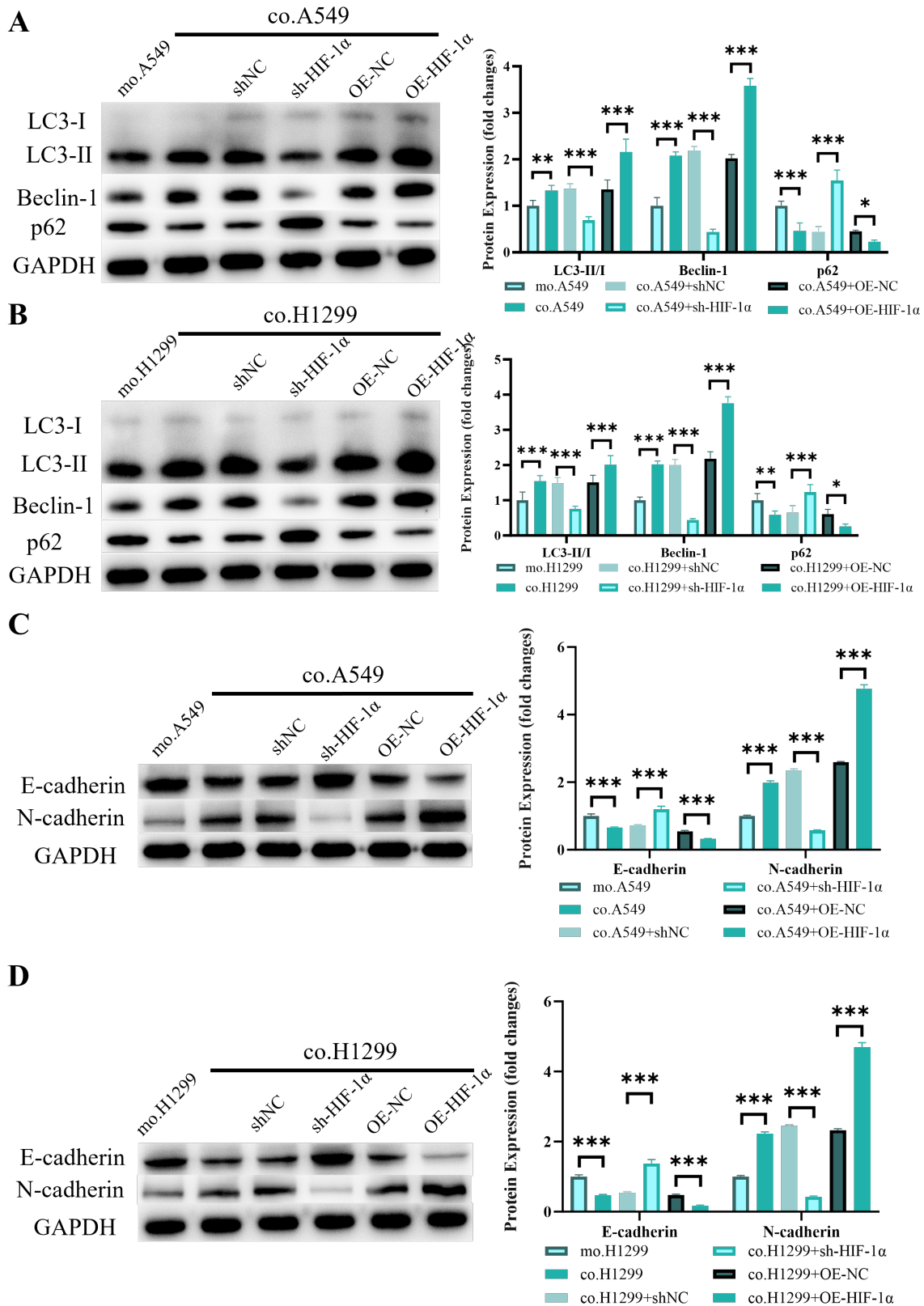


Fig. 11. LC-MSC induction of lung cancer cell autophagy and epithelial-mesenchymal transition (EMT) promotion through HIF-1 α upregulation. Autophagy-related LC3-II/I ratio, Beclin-1 protein, and p62 protein in (A) differently treated A549 cells (n = 5) and (B) differently treated H1299 cells (n = 5). EMT-related E-cadherin and N-cadherin in (C) differently treated A549 cells (n = 5) and (D) differently treated H1299 cells (n = 5). * $p < 0.05$, ** $p < 0.01$, *** $p < 0.001$.

images were photographed by confocal microscopy (objective: 200×; CKX53, Olympus, Tokyo, Japan).

In-Vivo Experiments

Nude BALB/c mice (aged 4–6 weeks and weighing 18–20 g) were obtained from Beijing Vital River Laboratory Animal Technology Co., Ltd. (Beijing, China) and raised in a specific pathogen free-level environment. A549 lung cancer cells (1×10^6 cells dissolved in 100 μ L PBS) were subcutaneously injected into the right dorsal flank of mice on day 0. Tumor growth was monitored periodically, and on day 14, the mice were randomly divided into groups as described in the Result section, with five mice in each group. Then, the mice were exposed to saline or TMZ (50 mg/kg) via oral gavage for 5 consecutive days. On day 19, the mice were euthanatized by CO₂ asphyxiation, and tumor tissues from mouse lungs were harvested and snap frozen in liquid nitrogen. The following formula was used for calculation: $V = (L \times W^2)/2$ (V: tumor volume, W: the short axis, and L: long axis).

Immunohistochemistry (IHC)

Parts of the harvested tumor tissues were fixed in 4 % PBS-saturated formaldehyde, paraffin-embedded, and sectioned at 5 μ m thickness. Then, the sections were stained by incubating with the antibody of Ki-67 (1:200 dilution, ab15580, Abcam, Cambridge, MA, USA) in accordance with the manufacturer's instruction. The slides with stained sections were imaged by the microscope (CKX53, Olympus, Tokyo, Japan) at 400× magnification, and the percentage of positively labeled cells was counted among more than 1000 tumor nuclei.

Terminal Deoxynucleotidyl Transferase-Mediated dUTP Nick End Labeling (TUNEL) Assay

TUNEL staining was performed using a kit (C1089, Beyotime, Shanghai, China) in accordance with the manufacturer's instructions, in which the green fluorescein labeled the apoptotic nuclei and the blue fluorescein marked the total cardiomyocyte nuclei (DAPI stained). The labeled tissues were viewed by microscopy (CKX53, Olympus, Tokyo, Japan).

RT-qPCR

Total RNA was extracted (TRIzol, 15596026, Invitrogen, Carlsbad, CA, USA) and reversely transcribed into cDNA by using Reverse Transcriptase (D7166, Beyotime, Shanghai, China). cDNA was amplified (FP207, TIAN-GEN Biotech, Beijing, China) under the following conditions: pre-denaturation (94 °C, 5 min) and 40 cycles of denaturation (94 °C, 10 s) followed by annealing (60 °C, 60 s). Glyceraldehyde-3-phosphate dehydrogenase (GAPDH) was used for normalization, and the $2^{-\Delta\Delta C_t}$ method was used for analyzing expression levels. The primer sequences are listed in Table 1.

Table 1. Primer sequences.

Name of primers	Sequences of primers (5'-3')
HIF-1 α -F	CTCAAAGTCGGACAGCCTCA
HIF-1 α -R	CCCTGCAGTAGGTTTCTGCT
GAPDH-F	ATGGGAGCTGGTCATCAAC
GAPDH-R	CCACAGTCTTCTGAGTGGCA

HIF-1 α , hypoxia-inducible factor-1 α ; GAPDH, glyceraldehyde-3-phosphate dehydrogenase.

Western Blot

Cell or tissue lysates were obtained using radioimmunoprecipitation assay (RIPA) lysis buffer (P0013, Beyotime, Shanghai, China) with the protease and phosphatase inhibitors (ST505, Beyotime, Shanghai, China) being added before use. After the cell lysates were centrifugated at 12,000 g for 15 min and the supernatants were collected, the total protein in the supernatants was quantified using the bicinchoninic acid kit (P0012, Beyotime, Shanghai, China). Proteins (50 μ g) were separated by sodium dodecyl sulfate (SDS)-polyacrylamide gel (10 %) and transferred onto a polyvinylidene fluoride membrane, which was then blocked with 5 % skim milk at 37 °C for 1 h. Subsequently, the membrane was incubated with primary antibodies purchased from Abcam (Cambridge, MA, USA) for HIF-1 α (1:2000 dilution, ab224689), LC3 (1:1000 dilution; ab62721), Beclin-1 (1:2000 dilution; ab207612), p62 (1:1000 dilution; ab91526), E-cadherin (1:1000 dilution; ab212059), N-cadherin (1:1000 dilution; ab98952), and GAPDH (1:2000 dilution; ab8245) at 4 °C overnight. The membrane was washed with Tris-buffered saline with Tween-20 (TBST) and probed with horseradish peroxidase-conjugated secondary antibodies (1:5000 dilution; ab205719, Abcam, Cambridge, MA, USA). After being washed with TBST, the immunoreactive bands were revealed using enhanced chemiluminescence (ECL, WP20005, Invitrogen, Carlsbad, CA, USA), and the intensities of the bands were quantified through Image-Pro Plus (version 6.0, Media Cybernetics, Rockville, CA, USA).

Statistical Analysis

Data were presented as the mean \pm standard deviation (SD). The difference between groups was analyzed using one-way analysis of variance with Tukey's post hoc test. $p < 0.05$ was considered statistically significant.

Results

Verification of Isolated LC-MSCs

A single-cell suspension of LC-MSCs was generated from lung cancer tissues, and the presumed LC-MSCs were characterized and verified in several manners. Under optical microscopy (Fig. 1A), the cells were firmly attached to the surface of plates, showing a fibroblast-like morphology. The cell proliferation rate was increased and maintained even at advanced passages, with no morphological changes.

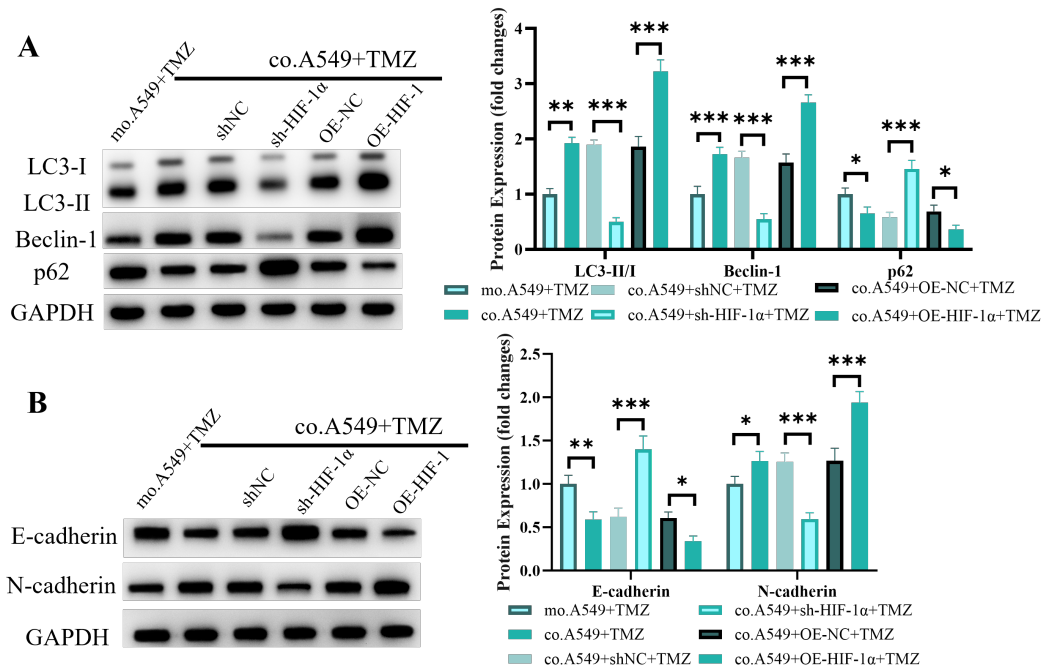


Fig. 12. LC-MSC induction of lung cancer cell autophagy and promotion of epithelial-mesenchymal transition (EMT) through HIF-1α upregulation and TMZ treatment. (A) Autophagy-related LC3-II/I ratio, Beclin-1 protein, and p62 protein expression levels in differently treated A549 cells (n = 5). (B) EMT-related E-cadherin and N-cadherin expression levels in differently treated A549 cells (n = 5). **p* < 0.05, ***p* < 0.01, ****p* < 0.001.

The expression levels of markers associated with LC-MSCs were determined by immunophenotyping via flow cytometry. As shown in Fig. 1B,C, the isolated cells were positive for CD29, CD73, CD105, and CD90 and negative for CD34, HLA-DR, CD14, and CD45, indicating the phenotype of MSC. The isolated cells could successfully differentiate into adipose cells, osteocytes, or chondrocytes by induction (Fig. 1D). These findings indicated that the LC-MSCs were successfully isolated.

Increase in the Progression and Chemoresistance of Lung Cancer Cells by LC-MSCs

The lung cancer cells were treated with different concentrations of TMZ. As shown in Fig. 2A, when no TMZ treatment was applied (0 μM), the lung cancer cells co-cultured with LC-MSCs proliferated more than the lung cancer cells cultured alone (*p* < 0.01), indicating that LC-MSCs could promote the proliferation of lung cancer cells. Moreover, when cells were treated with TMZ, the lung cancer cells co-cultured with LC-MSCs proliferated more than the lung cancer cells cultured alone (*p* < 0.001). Especially when the concentration of TMZ was 200 μM, the difference of proliferation rates between differently cultured lung cancer cells was the biggest. These findings demonstrated that LC-MSCs could enhance the chemoresistance of lung cancer cells against TMZ. The TMZ concentration of 200 μM was chosen for the subsequent experiments. As shown in Fig. 2B, co-culture with LC-MSCs led to decreased per-

centage of lung cancer cells in the G0/G1 phase (*p* < 0.05) and increased percentage of lung cancer cells in the S phase (*p* < 0.001) under or under no TMZ treatment, indicating that LC-MSCs promoted the proliferation and improved the chemoresistance of lung cancer cells. The assays for migration (Figs. 3A,B,4A) and invasion (Fig. 4B) demonstrated that under the conditions with or without TMZ treatment, the lung cancer cells co-cultured with LC-MSCs migrated and invaded more than the lung cancer cells cultured alone (*p* < 0.001). Fig. 5 shows that the LC-MSCs decreased the apoptosis (*p* < 0.001) of cells under or under no TMZ treatment. These findings suggested that LC-MSCs promoted the progression of lung cancer cells under normal condition and enhanced the chemoresistance of lung cancer cells under chemical drug treatment.

LC-MSC Upregulation of HIF-1α Expression

The results of RT-qPCR (Fig. 6A), Western blot (Fig. 6B) and immunofluorescence analysis (Fig. 6C) demonstrated that HIF-1α was significantly upregulated in lung cancer cells when co-cultured with LC-MSCs (*p* < 0.001).

LC-MSC Enhancement of Chemoresistance of Lung Cancer Cells through Upregulating HIF-1α

As shown in Fig. 7A,B, in A549 and H1299 cells, HIF-1α was successfully downregulated by sh-HIF-1α transfection (*p* < 0.01) and successfully upregulated by OE-HIF-1α transfection (*p* < 0.01). When treated

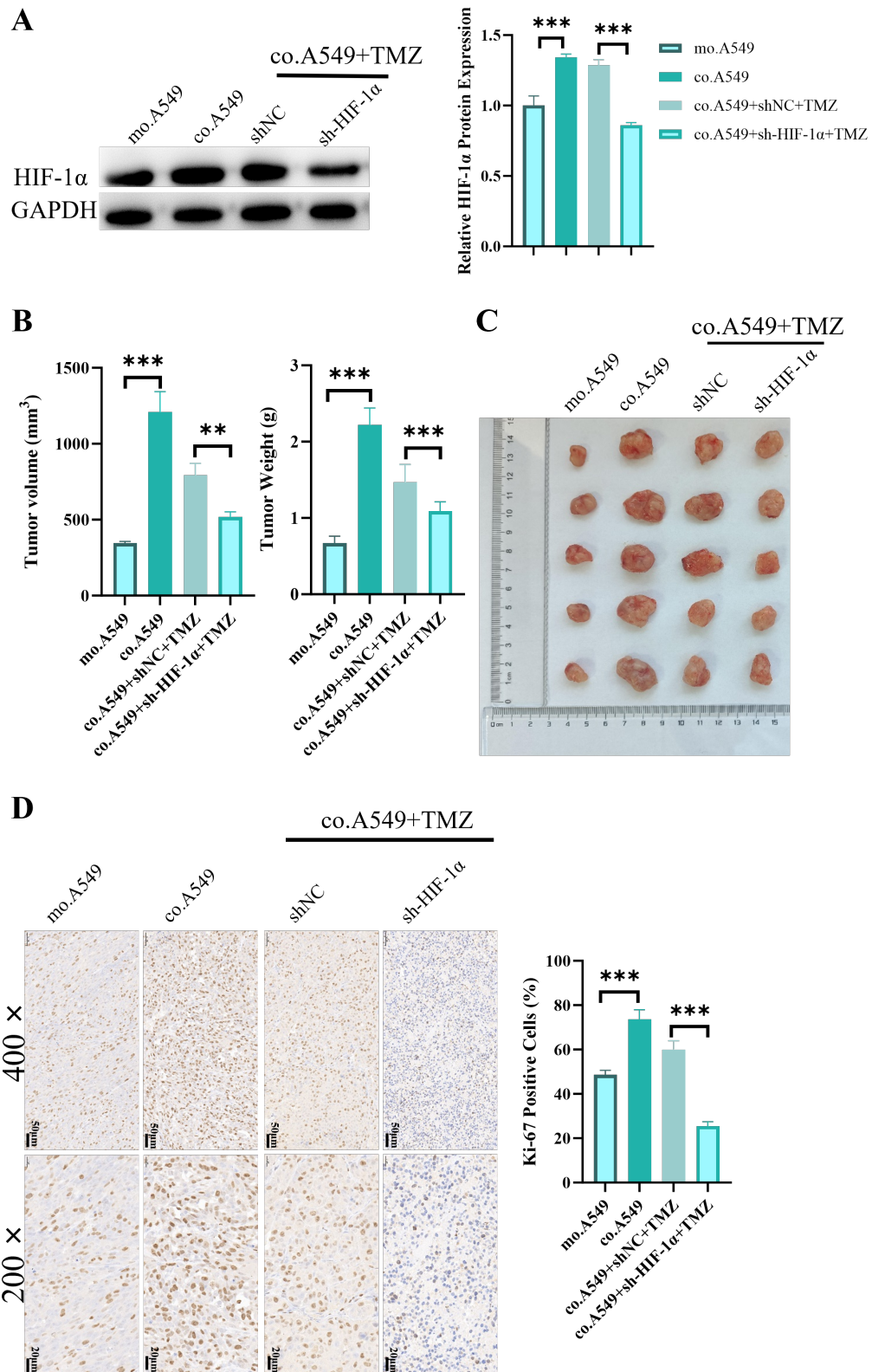


Fig. 13. LC-MSC promotion of the progression and chemoresistance of lung cancer *in vivo*. (A) HIF-1 α protein levels in lung cancer tumor tissues (n = 5). (B) Tumor volume and weight of lung cancer tumor tissues (n = 5). (C) Images of lung cancer tumor tissues. (D) Results of Ki-67 immunohistochemistry of lung cancer tumor tissues (n = 5; scale bar: 50 μ m for 400 \times , 20 μ m for 200 \times). ** p < 0.01, *** p < 0.001.

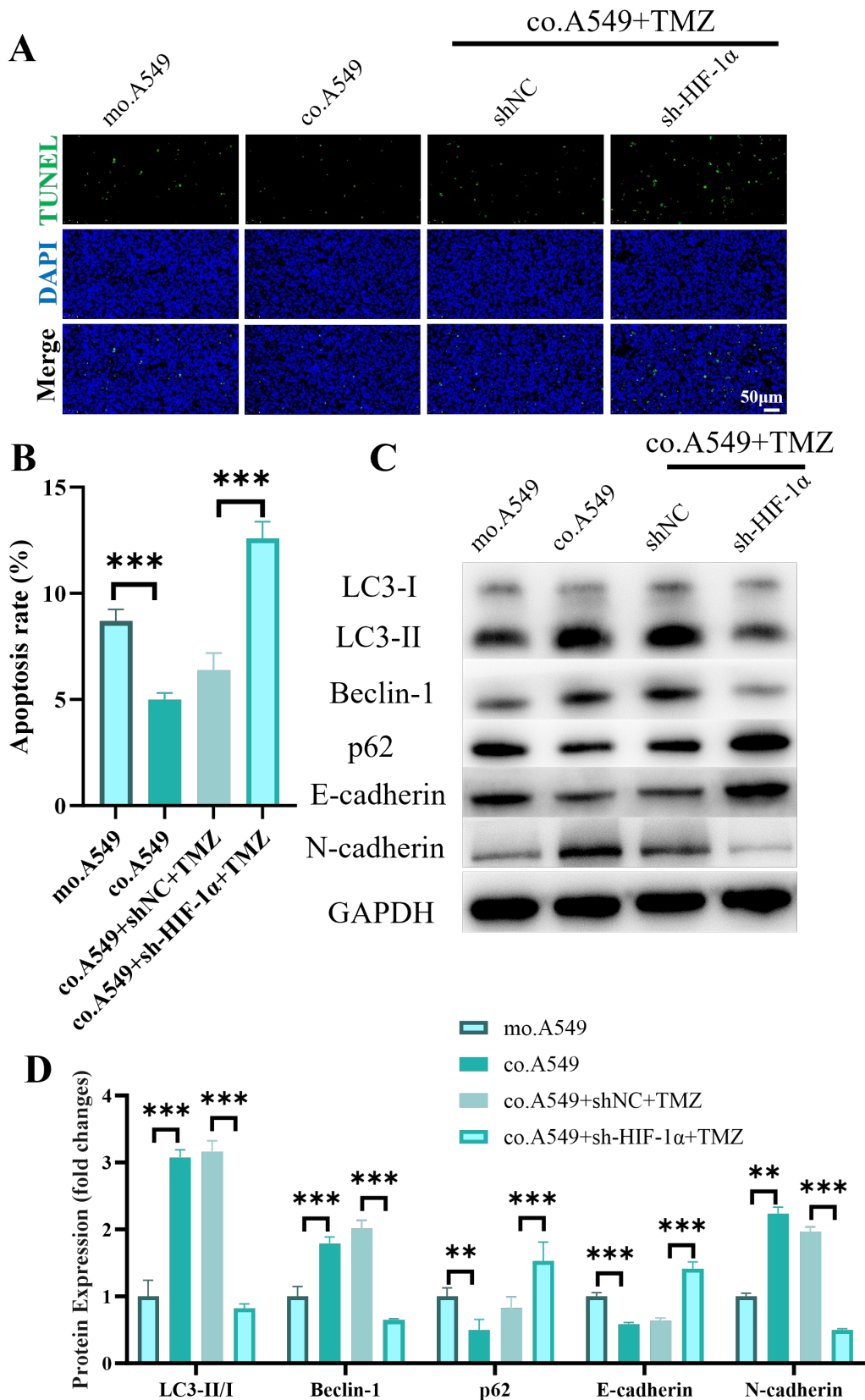


Fig. 14. LC-MSC promotion of the progression and chemoresistance of lung cancer *in vivo*. (A,B) TUNEL assay for lung cancer tumor tissues (n = 5; scale bar: 50 μ m). (C) Western blot images and (D) quantification of LC3-II/I ratio, Beclin-1, p62, E-cadherin, and N-cadherin (n = 5). ** $p < 0.01$, *** $p < 0.001$. TUNEL, terminal deoxynucleotidyl transferase-mediated dUTP nick end labeling.

with TMZ, the lung cancer cells (A549 and H1299 co-cultured with LC-MSCs) in which HIF-1 α was downregulated/upregulated proliferated less/more ($p < 0.001$) than the cells in which HIF-1 α was not regulated (Fig. 7C,D). As shown in Fig. 8A,B, in A549 and H1299 cells co-cultured with LC-MSCs, the downregulation of HIF-1 α increased the cell percentage of the G0/G1 phase ($p < 0.01$) and decreased that of the S phase ($p < 0.001$). Meanwhile, the upregulation of HIF-1 α decreased the percentage of cells in the G0/G1 phase ($p < 0.001$) and increased that in the S phase ($p < 0.05$). These findings suggested that HIF-1 α could promote the proliferation of lung cancer cells treated with TMZ. When co-cultured with LC-MSCs and treated with TMZ, the lung cancer cells in which HIF-1 α was downregulated/upregulated migrated less/more (Fig. 9A–D, $p < 0.001$), were invaded less/more (Fig. 10A,B, $p < 0.001$), and died due to apoptosis more/less (Fig. 10C,D, $p < 0.001$) than the cells in which HIF-1 α was not regulated. All these findings suggested that when co-cultured with LC-MSCs, the chemoresistance of lung cancer cells against TMZ was enhanced by the LC-MSCs upregulating HIF-1 α .

LC-MSC Induction of Autophagy of Lung Cancer Cells and Promotion of EMT through Upregulating HIF-1 α

As shown in Fig. 11A,B, when lung cancer cells were co-cultured with LC-MSCs, in which HIF-1 α was up-regulated as shown above, the Beclin-1 expression and LC3-II/I ratio were increased ($p < 0.01$) and p62 expression was decreased ($p < 0.01$). Furthermore, the Beclin-1 expression and LC3-II/I ratio were decreased ($p < 0.001$) and p62 expression was increased ($p < 0.001$) in LC-MSC-co-cultured lung cancer cells with HIF-1 α downregulated. Meanwhile, the LC3-II/I ratio and Beclin-1 expression were increased ($p < 0.001$) and p62 expression was decreased ($p < 0.001$) in LC-MSC-co-cultured lung cancer cells and with HIF-1 α upregulated. These changes in proteins related to autophagy demonstrated that LC-MSCs induced autophagy in lung cancer cells through upregulating HIF-1 α expression. The effect of LC-MSCs on epithelial-mesenchymal transition (EMT) is shown in Fig. 11C,D. When lung cancer cells were co-cultured with LC-MSCs, in which HIF-1 α was upregulated as shown above, E-cadherin expression was decreased ($p < 0.001$) and N-cadherin expression was increased ($p < 0.001$). On the contrary, E-cadherin expression was increased ($p < 0.001$) and N-cadherin expression was decreased ($p < 0.001$) in LC-MSC-co-cultured lung cancer cells and with HIF-1 α downregulated, whereas E-cadherin expression was decreased ($p < 0.001$) and N-cadherin expression was increased ($p < 0.001$) in LC-MSC-co-cultured lung cancer cells and with HIF-1 α upregulated. These changes in EMT-related proteins demonstrated that LC-MSCs induced EMT in lung cancer cells through upregulating HIF-1 α expression. TMZ was then used to intervene, and the results in Fig. 12A,B

showed that the LC3-II/I ratio and Beclin-1 expression significantly increased ($p < 0.001$) and p62 expression significantly decreased ($p < 0.05$) after HIF-1 α overexpression in co.A549 cells. Meanwhile, N-cadherin expression increased significantly, whereas E-cadherin expression decreased significantly. These results suggested that LC-MSCs promote chemotherapy resistance by upregulating HIF-1 α expression ($p < 0.001$).

LC-MSC Promotion of Progression and Chemoresistance in Lung Cancer In Vivo

Fig. 13A shows that compared with the tumor formed by lung cancer cells, the tumors formed from lung cancer cells with LC-MSCs had upregulated HIF-1 α ($p < 0.001$). Meanwhile, HIF-1 α was downregulated in tumors formed from HIF-1 α downregulated lung cancer cells with LC-MSCs and treated with TMZ ($p < 0.001$). As shown in Fig. 13B,C, the volume and weight of the tumor formed from lung cancer cells with LC-MSCs increased ($p < 0.001$), indicating that LC-MSCs promoted lung cancer tumor growth. In tumors formed from lung cancer cells with LC-MSCs, the growth was more inhibited by TMZ when HIF-1 α was downregulated ($p < 0.01$). The result of Ki-67 immunohistochemical analysis shown in Fig. 13D demonstrated that Ki-67-positive cells were more presented in tumors formed from lung cancer cells with LC-MSCs ($p < 0.001$). When treated with TMZ, the Ki-67-positive cells were less presented in tumors formed from HIF-1 α -downregulated lung cancer cells with LC-MSCs ($p < 0.001$). Fig. 14A–D shows decreased cell apoptosis ($p < 0.001$), p62 protein expression ($p < 0.01$), and E-cadherin expression ($p < 0.001$) and increased LC3-II/I ratio ($p < 0.001$), Beclin-1 expression ($p < 0.01$), and N-cadherin expression ($p < 0.01$), indicating that LC-MSCs could promote induce autophagy and EMT in lung cancer and suppress apoptosis in tumor cells. When treated with TMZ, the cell apoptosis ($p < 0.001$), p62 protein expression ($p < 0.001$), and E-cadherin expression ($p < 0.001$) increased, whereas the LC3-II/I ratio ($p < 0.001$), Beclin-1 expression ($p < 0.01$), and N-cadherin expression ($p < 0.001$) decreased in tumors formed from HIF-1 α downregulated lung cancer cells with LC-MSCs. All these findings indicated that LC-MSCs promote tumor growth and chemoresistance through upregulating the expression of HIF-1 α .

Discussion

In this study, MSCs were successfully isolated from lung cancer tissues, and whether they could facilitate the progression and chemoresistance of lung cancer through mediating the expression of HIF-1 α was verified.

At present, the MSCs used for clinical applications are mainly from cord blood, bone marrow, and adipose tissues, which are obtained from birth-derived tissues by aspiration and liposuction [21]. In the present study, MSCs isolated from lung cancer tissues were used to reveal how

exactly MSCs residing in lung cancer tissues affect the development of lung cancer. MSCs have been commonly accepted to be capable of inhibiting the development of tumors by various mechanisms, including tumor cell cycle jeopardization and apoptosis induction [22]. The present study demonstrated that the LC-MSCs had pro-tumor functions for lung cancer *in vitro* and *in vivo*, consistent with the results of a previous study [23]. Lung cancer cells co-cultured with LC-MSCs possessed higher ability of progression, including more proliferation, migration, and invasion and less apoptosis, than lung cancer cells cultured alone. TMZ is considered as a treatment for several solid tumors such as melanoma, neuroendocrine tumor, sarcomas, glioblastoma, and glioma [24–30]. It has been proven to act against lung cancer progression [31,32]. In the present study, when lung cancer cells were co-cultured with LC-MSCs, their drug resistance against TMZ significantly increased, presenting more proliferation, migration, and invasion and less apoptosis.

The underlying mechanisms by which LC-MSCs promote lung cancer progression were explored. MSCs could regulate various signaling pathways related to cancer initiation and progression [33]. In the present study, when lung cancer cells were cultured with LC-MSCs, the HIF-1 α expression in cells increased. HIF-1 α was proven by numerous previous studies to be associated with the progression of lung cancer [34–37]. In the present study, it was proven to be related to the drug resistance of lung cancer cells against TMZ. The PI3K/Akt/HIF-1 α pathway is believed to be related to lung cancer [38,39]. It has been proven to be modulated by MSCs and to enhance the progression of cancers [40,41]. The modulation of LC-MSCs on HIF-1 α could be based on the PI3K/Akt pathway, which could be explored further. Moreover, NF- κ B may be involved in this modulation mechanism because NF- κ B/HIF-1 α has been proven to be related to lung cancer progression [42]. NF- κ B plays a role in EMT and tumor metastasis, consistent with the finding that EMT was regulated by HIF-1 α mediated by LC-MSCs. Furthermore, the EMT hallmark of downregulated E-cadherin expression and upregulated N-cadherin expression is considered as a common signature for carcinogenesis and wound healing [43], further proving the promotive effect of LC-MSCs and its upregulated HIF-1 α on the progression of lung cancer. Meanwhile, LC-MSCs mediating HIF-1 α could promote lung cancer progression, and HIF could mediate the tumor homing of MSCs [44]. Therefore, the crosstalk between LC-MSCs and HIF-1 α in affecting lung cancer needs further investigation.

Previous studies revealed that HIF-1 α induced autophagy and conferred the chemoresistance of cancer cell [45,46]. Autophagy could regulate the response to stress and maintain homeostasis, facilitating the development and chemoresistance of cancer [47,48]. In the present study, when HIF-1 α was determined to induce autophagy, it was also determined to inhibit apoptosis, which is a well-known

mechanism by which chemoresistance develops. These findings proved that LC-MSCs could promote the progression and chemoresistance of lung cancer through mediating HIF-1 α expression.

This study still has many shortcomings. No clinical samples were used for further investigation. Only two cell lines were used in this study, and more cell lines should be used in the future to validate the existing conclusions.

Conclusions

LC-MSCs promote the malignant progression of lung cancer and enhance cancer cell resistance to chemotherapy through upregulating the expression of HIF-1 α , which further mediates cancer cell proliferation, metastasis, apoptosis, and autophagy. This study provides new targets for MSC-based therapeutic strategies for lung cancer, thus facilitating the optimization of lung cancer treatment.

List of Abbreviations

MSCs, mesenchymal stem cells; LC-MSCs, lung cancer-associated mesenchymal stem cells; TMZ, temozolomide; HIF-1 α , hypoxia-inducible factor-1 α ; EMT, epithelial-mesenchymal transition; TUNEL, terminal deoxynucleotidyl transferase-mediated dUTP nick end labeling; RT-qPCR, reverse transcription quantitative polymerase chain reaction; ECL, enhanced chemiluminescence; PBS, phosphate-buffered saline; DMEM, Dulbecco's modified Eagle medium; FBS, fetal bovine serum; TGF, transforming growth factor; CCK, cell counting kit; PI, propidium; DAPI, 2-(4-amidinophenyl)-6-indolecarbamidine dihydrochloride; GAPDH, glyceraldehyde-3-phosphate dehydrogenase; TBST, Tris-buffered saline with Tween-20; SD, standard deviation; sh, short hairpin; shNC, noncoding shRNA; OE, overexpression; IHC, immunohistochemistry.

Availability of Data and Materials

The datasets used and/or analysed during the current study were available from the corresponding author on reasonable request.

Author Contributions

LBP and JL designed the study. ZWZ and JL collected and analyzed the data. LBP and CQZ participated in drafting the manuscript. All authors conducted the study and contributed to critical revision of the manuscript for important intellectual content. All authors gave final approval of the version to be published. All authors participated fully in the work, took public responsibility for appropriate portions of the content, and agreed to be accountable for all aspects of the work in ensuring that questions related to the accuracy or completeness of any part of the work were appropriately investigated and resolved.

Ethics Approval and Consent to Participate

All animal procedures were performed in accordance with the Guidelines for the Care and Use of Laboratory Animals of Jinan Central Hospital. The study was approved by the Institutional Animal Care and Use Committee of Jinan Central Hospital (Approval No. JNCHIAUC2024-16). This study was approved by the Ethics Committee of Jinan Central Hospital (institution review board number, R202403040120). This study was performed in accordance with the principles of the Declaration of Helsinki. Informed consent has been obtained from all participants involved in the study.

Acknowledgments

Not applicable.

Funding

Not applicable.

Conflict of Interest

The authors declare no conflict of interest.

References

- Nooreldeen R, Bach H. Current and Future Development in Lung Cancer Diagnosis. *International Journal of Molecular Sciences*. 2021; 22: 8661. <https://doi.org/10.3390/ijms22168661>.
- Bray F, Ferlay J, Soerjomataram I, Siegel RL, Torre LA, Jemal A. Global cancer statistics 2018: GLOBOCAN estimates of incidence and mortality worldwide for 36 cancers in 185 countries. *CA: A Cancer Journal for Clinicians*. 2018; 68: 394–424. <https://doi.org/10.3322/caac.21492>.
- Torre LA, Bray F, Siegel RL, Ferlay J, Lortet-Tieulent J, Jemal A. Global cancer statistics, 2012. *CA: A Cancer Journal for Clinicians*. 2015; 65: 87–108. <https://doi.org/10.3322/caac.21262>.
- Henschke CI, International Early Lung Cancer Action Program Investigators. Survival of patients with clinical stage I lung cancer diagnosed by computed tomography screening for lung cancer. *Clinical Cancer Research: an Official Journal of the American Association for Cancer Research*. 2007; 13: 4949–4950. <https://doi.org/10.1158/1078-0432.Ccr-07-0317>.
- Warren GW, Ostroff JS, Goffin JR. Lung Cancer Screening, Cancer Treatment, and Addressing the Continuum of Health Risks Caused by Tobacco. *American Society of Clinical Oncology Educational Book/ASCO*. 2016; 35: 223–229. https://doi.org/10.1200/edbk_158704.
- Casagrande GMS, Silva MO, Reis RM, Leal LF. Liquid Biopsy for Lung Cancer: Up-to-Date and Perspectives for Screening Programs. *International Journal of Molecular Sciences*. 2023; 24: 2505. <https://doi.org/10.3390/ijms24032505>.
- Sun Y, Shen W, Hu S, Lyu Q, Wang Q, Wei T, *et al.* METTL3 promotes chemoresistance in small cell lung cancer by inducing mitophagy. *Journal of Experimental & Clinical Cancer Research: CR*. 2023; 42: 65. <https://doi.org/10.1186/s13046-023-02638-9>.
- Farago AF, Keane FK. Current standards for clinical management of small cell lung cancer. *Translational Lung Cancer Research*. 2018; 7: 69–79. <https://doi.org/10.21037/tlcr.2018.01.16>.
- Gazdar AF, Bunn PA, Minna JD. Small-cell lung cancer: what we know, what we need to know and the path forward. *Nature Reviews. Cancer*. 2017; 17: 725–737. <https://doi.org/10.1038/nrc.2017.87>.
- Friedenstein AJ, Gorskaja JF, Kulagina NN. Fibroblast precursors in normal and irradiated mouse hematopoietic organs. *Experimental Hematology*. 1976; 4: 267–274.
- Fukuchi Y, Nakajima H, Sugiyama D, Hirose I, Kitamura T, Tsuji K. Human placenta-derived cells have mesenchymal stem/progenitor cell potential. *Stem Cells*. 2004; 22: 649–658. <https://doi.org/10.1634/stemcells.22-5-649>.
- Li Z, Hu X, Zhong JF. Mesenchymal Stem Cells: Characteristics, Function, and Application. *Stem Cells International*. 2019; 2019: 8106818. <https://doi.org/10.1155/2019/8106818>.
- Lv FJ, Tuan RS, Cheung KM, Leung VY. Concise review: the surface markers and identity of human mesenchymal stem cells. *Stem Cells*. 2014; 32: 1408–1419. <https://doi.org/10.1002/stem.1681>.
- Brinkhof B, Zhang B, Cui Z, Ye H, Wang H. *ALCAM* (CD166) as a gene expression marker for human mesenchymal stromal cell characterisation. *Gene*. 2020; 763s: 100031. <https://doi.org/10.1016/j.gene.2020.100031>.
- De Becker A, Riet IV. Homing and migration of mesenchymal stromal cells: How to improve the efficacy of cell therapy? *World Journal of Stem Cells*. 2016; 8: 73–87. <https://doi.org/10.4252/wjsc.v8.i3.73>.
- Naji A, Eitoku M, Favier B, Deschaseaux F, Rouas-Freiss N, Sukanuma N. Biological functions of mesenchymal stem cells and clinical implications. *Cellular and Molecular Life Sciences: CMLS*. 2019; 76: 3323–3348. <https://doi.org/10.1007/s00018-019-03125-1>.
- Ridge SM, Sullivan FJ, Glynn SA. Mesenchymal stem cells: key players in cancer progression. *Molecular Cancer*. 2017; 16: 31. <https://doi.org/10.1186/s12943-017-0597-8>.
- Hmadcha A, Martin-Montalvo A, Gauthier BR, Soria B, Capilla-Gonzalez V. Therapeutic Potential of Mesenchymal Stem Cells for Cancer Therapy. *Frontiers in Bioengineering and Biotechnology*. 2020; 8: 43. <https://doi.org/10.3389/fbioe.2020.00043>.
- Yan C, Chang J, Song X, Qi Y, Ji Z, Liu T, *et al.* Lung cancer-associated mesenchymal stem cells promote tumor metastasis and tumorigenesis by induction of epithelial-mesenchymal transition and stem-like reprogram. *Aging*. 2021; 13: 9780–9800. <https://doi.org/10.18632/aging.202732>.
- Khatri M, O'Brien TD, Chattha KS, Saif LJ. Porcine lung mesenchymal stromal cells possess differentiation and immunoregulatory properties. *Stem Cell Research & Therapy*. 2015; 6: 222. <https://doi.org/10.1186/s13287-015-0220-0>.
- Berebichez-Fridman R, Montero-Olvera PR. Sources and Clinical Applications of Mesenchymal Stem Cells: State-of-the-art review. *Sultan Qaboos University Medical Journal*. 2018; 18: e264–e277. <https://doi.org/10.18295/squmj.2018.18.03.002>.
- Fathi E, Sanaat Z, Farahzadi R. Mesenchymal stem cells in acute myeloid leukemia: a focus on mechanisms involved and therapeutic concepts. *Blood Research*. 2019; 54: 165–174. <https://doi.org/10.5045/br.2019.54.3.165>.
- Galland S, Stamenkovic I. Mesenchymal stromal cells in cancer: a review of their immunomodulatory functions and dual effects on tumor progression. *The Journal of Pathology*. 2020; 250: 555–572. <https://doi.org/10.1002/path.5357>.
- Stupp R, Brada M, van den Bent MJ, Tonn JC, Pentheroudakis G, ESMO Guidelines Working Group. High-grade glioma: ESMO Clinical Practice Guidelines for diagnosis, treatment and follow-up. *Annals of Oncology: Official Journal of the European Society for Medical Oncology/ESMO*. 2014; 25: iii93–iii101. <https://doi.org/10.1093/annonc/mdu050>.
- Pavel M, Öberg K, Falconi M, Krenning EP, Sundin A, Perren A, *et al.* Gastroenteropancreatic neuroendocrine neoplasms: ESMO Clinical Practice Guidelines for diagnosis, treatment and follow-up. *Annals of Oncology: Official Journal of the European Society for Medical Oncology/ESMO*. 2020; 31: 844–860. <https://doi.org/10.1016/j.annonc.2020.03.304>.
- Swetter SM, Thompson JA, Albertini MR, Barker CA, Baumgartner J, Boland G, *et al.* NCCN Guidelines® Insights: Melanoma: Cutaneous

- neous, Version 2.2021. Journal of the National Comprehensive Cancer Network: JNCCN. 2021; 19: 364–376. <https://doi.org/10.6004/jnccn.2021.0018>.
- [27] von Mehren M, Kane JM, Bui MM, Choy E, Connelly M, Dry S, *et al.* NCCN Guidelines Insights: Soft Tissue Sarcoma, Version 1.2021. Journal of the National Comprehensive Cancer Network: JNCCN. 2020; 18: 1604–1612. <https://doi.org/10.6004/jnccn.2020.0058>.
- [28] Casali PG, Bielack S, Abecassis N, Aro HT, Bauer S, Biagini R, *et al.* Bone sarcomas: ESMO-PaedCan-EURACAN Clinical Practice Guidelines for diagnosis, treatment and follow-up. Annals of Oncology: Official Journal of the European Society for Medical Oncology/ESMO. 2018; 29: iv79–iv95. <https://doi.org/10.1093/annonc/mdy310>.
- [29] Nabors LB, Portnow J, Ahluwalia M, Baehring J, Brem H, Brem S, *et al.* Central Nervous System Cancers, Version 3.2020, NCCN Clinical Practice Guidelines in Oncology. Journal of the National Comprehensive Cancer Network: JNCCN. 2020; 18: 1537–1570. <https://doi.org/10.6004/jnccn.2020.0052>.
- [30] Gronchi A, Miah AB, Dei Tos AP, Abecassis N, Bajpai J, Bauer S, *et al.* Soft tissue and visceral sarcomas: ESMO-EURACAN-GENTURIS Clinical Practice Guidelines for diagnosis, treatment and follow-up. Annals of Oncology: Official Journal of the European Society for Medical Oncology/ESMO. 2021; 32: 1348–1365. <https://doi.org/10.1016/j.annonc.2021.07.006>.
- [31] Gomez-Gutierrez JG, Nitz J, Sharma R, Wechman SL, Riedinger E, Martinez-Jaramillo E, *et al.* Combined therapy of oncolytic adenovirus and temozolomide enhances lung cancer virotherapy *in vitro* and *in vivo*. Virology. 2016; 487: 249–259. <https://doi.org/10.1016/j.virol.2015.10.019>.
- [32] Hamzawy MA, Abo-Youssef AM, Salem HF, Mohammed SA. Antitumor activity of intratracheal inhalation of temozolomide (TMZ) loaded into gold nanoparticles and/or liposomes against urethane-induced lung cancer in BALB/c mice. Drug Delivery. 2017; 24: 599–607. <https://doi.org/10.1080/10717544.2016.1247924>.
- [33] Torsvik A, Bjerkvig R. Mesenchymal stem cell signaling in cancer progression. Cancer Treatment Reviews. 2013; 39: 180–188. <https://doi.org/10.1016/j.ctrv.2012.03.005>.
- [34] Hua Q, Mi B, Xu F, Wen J, Zhao L, Liu J, *et al.* Hypoxia-induced lncRNA-AC020978 promotes proliferation and glycolytic metabolism of non-small cell lung cancer by regulating PKM2/HIF-1 α axis. Theranostics. 2020; 10: 4762–4778. <https://doi.org/10.7150/thno.43839>.
- [35] Hao S, Li F, Jiang P, Gao J. Effect of chronic intermittent hypoxia-induced HIF-1 α /ATAD2 expression on lung cancer stemness. Cellular & Molecular Biology Letters. 2022; 27: 44. <https://doi.org/10.1186/s11658-022-00345-5>.
- [36] Huang Y, Chen Z, Lu T, Bi G, Li M, Liang J, *et al.* HIF-1 α switches the functionality of TGF- β signaling via changing the partners of smads to drive glucose metabolic reprogramming in non-small cell lung cancer. Journal of Experimental & Clinical Cancer Research: CR. 2021; 40: 398. <https://doi.org/10.1186/s13046-021-02188-y>.
- [37] Chen Z, Hu Z, Sui Q, Huang Y, Zhao M, Li M, *et al.* lncRNA FAM83A-AS1 facilitates tumor proliferation and the migration via the HIF-1 α / glycolysis axis in lung adenocarcinoma. International Journal of Biological Sciences. 2022; 18: 522–535. <https://doi.org/10.7150/ijbs.67556>.
- [38] Liu X, Liu L, Chen K, Sun L, Li W, Zhang S. Huaier shows anticancer activities by inhibition of cell growth, migration and energy metabolism in lung cancer through PI3K/AKT/HIF-1 α pathway. Journal of Cellular and Molecular Medicine. 2021; 25: 2228–2237. <https://doi.org/10.1111/jcmm.16215>.
- [39] Wan J, Wu W, Chen Y, Kang N, Zhang R. Insufficient radiofrequency ablation promotes the growth of non-small cell lung cancer cells through PI3K/Akt/HIF-1 α signals. Acta Biochimica et Biophysica Sinica. 2016; 48: 371–377. <https://doi.org/10.1093/abbs/gmw005>.
- [40] Yan XL, Fu CJ, Chen L, Qin JH, Zeng Q, Yuan HF, *et al.* Mesenchymal stem cells from primary breast cancer tissue promote cancer proliferation and enhance mammosphere formation partially via EGF/EGFR/Akt pathway. Breast Cancer Research and Treatment. 2012; 132: 153–164. <https://doi.org/10.1007/s10549-011-1577-0>.
- [41] Liu C, Feng X, Wang B, Wang X, Wang C, Yu M, *et al.* Bone marrow mesenchymal stem cells promote head and neck cancer progression through Periostin-mediated phosphoinositide 3-kinase/Akt/mammalian target of rapamycin. Cancer Science. 2018; 109: 688–698. <https://doi.org/10.1111/cas.13479>.
- [42] Li J, Zhang J, Xie F, Peng J, Wu X. Macrophage migration inhibitory factor promotes Warburg effect via activation of the NF- κ B/HIF-1 α pathway in lung cancer. International Journal of Molecular Medicine. 2018; 41: 1062–1068. <https://doi.org/10.3892/ijmm.2017.3277>.
- [43] Shash LS, Ibrahim RA, Elgohary SA. E-cadherin and N-cadherin Immunohistochemical Expression in Proliferating Urothelial Lesions: Potential Novel Cancer Predictive EMT Profiles. Applied Immunohistochemistry & Molecular Morphology: AIMM/Official Publication of the Society for Applied Immunohistochemistry. 2021; 29: 657–666. <https://doi.org/10.1097/pai.0000000000000940>.
- [44] Lan T, Luo M, Wei X. Mesenchymal stem/stromal cells in cancer therapy. Journal of Hematology & Oncology. 2021; 14: 195. <https://doi.org/10.1186/s13045-021-01208-w>.
- [45] Lin SC, Chien CW, Lee JC, Yeh YC, Hsu KF, Lai YY, *et al.* Suppression of dual-specificity phosphatase-2 by hypoxia increases chemoresistance and malignancy in human cancer cells. The Journal of Clinical Investigation. 2011; 121: 1905–1916. <https://doi.org/10.1172/jci44362>.
- [46] Chen J, Kobayashi M, Darmanin S, Qiao Y, Gully C, Zhao R, *et al.* Pim-1 plays a pivotal role in hypoxia-induced chemoresistance. Oncogene. 2009; 28: 2581–2592. <https://doi.org/10.1038/onc.2009.124>.
- [47] Saha S, Panigrahi DP, Patil S, Bhutia SK. Autophagy in health and disease: A comprehensive review. Biomedicine & Pharmacotherapy = Biomédecine & Pharmacothérapie. 2018; 104: 485–495. <https://doi.org/10.1016/j.biopha.2018.05.007>.
- [48] Huang Z, Zhou L, Chen Z, Nice EC, Huang C. Stress management by autophagy: Implications for chemoresistance. International Journal of Cancer. 2016; 139: 23–32. <https://doi.org/10.1002/ijc.29990>.

Editor’s note: The Scientific Editor responsible for this paper was Yang Liu.

Received: 26th September 2024; **Accepted:** 18th December 2024; **Published:** 24th April 2025